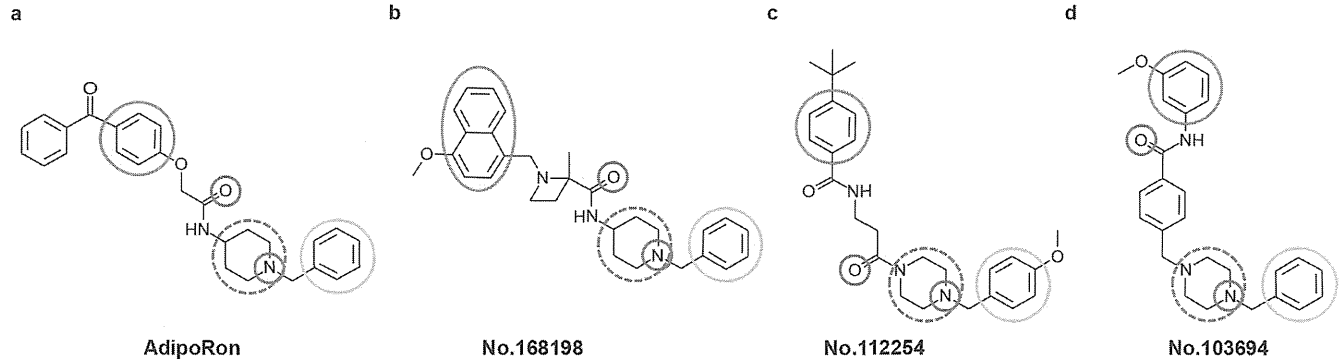

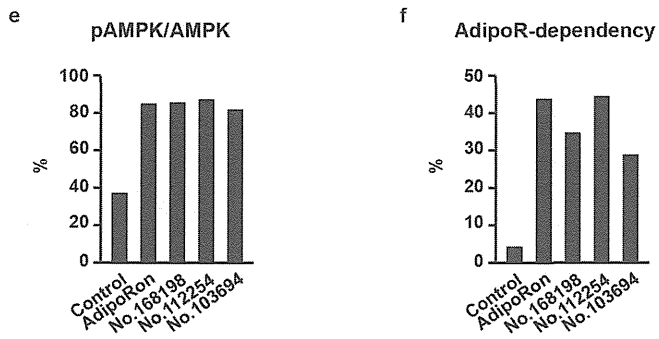

Extended Data Figure 8 | Chemical structures and AdipoR dependency of AMPK activation. a–d, Chemical structures of AdipoRon (**a**), compound 168198 (**b**), compound 112254 (**c**) and compound 103694 (**d**). Within the 1-benzyl 4-substituted 6-membered cyclic amine moiety, the cyclic amine moiety is surrounded by a dashed red circle, and the aromatic ring is surrounded by a light green circle. Cyan and dark green circles surround the carbonyl group and the terminal aromatic ring, respectively, located on the opposite side from the benzyl cyclic amine. **e**, Phosphorylation and amount of AMPK in C2C12 myotubes treated for 5 min with the indicated small-molecule compounds. Phosphorylation and amount of AMPK in C2C12 myotubes, treated for 5 min with the indicated small-molecule compounds (10 μM) (% relative to adiponectin). **f**, AdipoR dependency of AMPK activation. Phosphorylation and amount of AMPK in C2C12 myotubes and transfected with or without the AdipoR1 siRNA duplex, treated for 5 min with the indicated small molecule. AdipoR-dependency ratios were obtained by the following equation: 100 − (ratio for those transfected with the AdipoR1 siRNA duplex/ratio for those transfected without the AdipoR1 siRNA duplex) × 100 (%).

Extended Data Table 1 | Values of phosphorylation of AMPK in C2C12 myotubes

Compounds	%	Compounds	%	Compounds	%	Compounds	%	Compounds	%
Control	36.30	No.171076	48.67	No.197223	44.83	No.266924	40.60	No.354443	59.29
No.100491	37.78	No.171273	57.93	No.197248	89.63	No.267205	29.40	No.357301	59.19
No.101000	29.90	No.171723	97.60	No.197372	85.37	No.267582	30.14	No.359754	59.41
No.101138	34.34	No.171819	91.59	No.197491	69.57	No.267776	48.86	No.360919	40.83
No.101405	33.22	No.172743	53.55	No.197813	52.64	No.267789	25.70	No.362248	49.13
No.101962	88.84	No.175578	61.50	No.198204	44.15	No.267869	40.20	No.404565	41.91
No.102580	42.12	No.176916	67.27	No.198376	68.64	No.268037	73.29	No.406019	46.57
No.103264	36.58	No.178427	53.14	No.198637	87.39	No.268228	77.07	No.407905	44.57
No.103437	44.36	No.180655	52.89	No.198666	40.14	No.268472	35.97	No.408870	66.72
No.103694	81.05	No.180717	59.98	No.198962	55.06	No.268508	80.12	No.410887	48.29
No.106219	50.39	No.181166	79.96	No.200475	76.10	No.268915	53.61	No.411310	79.06
No.106449	45.13	No.181363	51.57	No.200737	83.71	No.268949	86.36	No.417441	39.23
No.107512	64.56	No.181432	86.82	No.201514	73.48	No.269553	49.33	No.421884	41.55
No.108049	84.33 #	No.181773	58.92	No.202274	45.61	No.269623	54.80	No.424954	33.68
No.108598	74.32	No.182007	67.31	No.202786	77.72	No.269969	42.64	No.427115	72.84
No.108693	67.68	No.182222	77.05	No.206685	90.15	No.269990	34.92	No.431183	77.01
No.112254	86.43 ##	No.182368	104.02	No.209705	81.28	No.270703	41.94	No.431986	60.80
No.113847	75.21	No.182410	76.46	No.211156	93.79	No.271038	60.07	No.434736	62.35
No.114755	67.02	No.182955	63.72	No.211636	39.43	No.271646	75.51	No.440150	54.14
No.115629	63.93	No.183257	57.18	No.211961	45.49	No.272007	47.33	No.440885	41.80
No.116956	70.23	No.183366	60.28	No.214221	45.73	No.272299	91.22	No.445174	47.63
No.117631	55.13	No.183406	58.30	No.214617	91.97	No.272350	84.20	No.445826	66.56
No.119375	53.30	No.183665	99.03	No.214991	76.02	No.272896	76.26	No.448315	58.34
No.125029	50.25	No.183910	57.14	No.216012	39.64	No.273574	61.28	No.449876	43.06
No.138809	49.79	No.183953	68.48	No.216801	36.89	No.274245	54.11	No.456699	49.34
No.138979	40.60	No.185321	63.03	No.217256	74.01	No.274971	81.64	No.456855	39.85
No.141020	39.04	No.185742	58.62	No.218325	50.36	No.275212	61.99	No.457274	49.00
No.141262	59.92	No.185747	73.20	No.238378	35.16	No.275297	56.55	No.457678	45.26
No.141317	36.80	No.186044	74.11	No.251327	83.18	No.275726	34.88	No.461226	52.94
No.141658	35.31	No.186101	66.82	No.253763	43.85	No.276027	34.47	No.462197	59.02
No.144387	47.92	No.186324	66.83	No.254620	34.68	No.276447	47.99	No.463825	68.63
No.144911	39.80	No.186681	49.05	No.255161	36.59	No.277217	47.80	No.466151	89.26
No.145329	44.22	No.187113	58.10	No.255518	56.12	No.278366	43.35	No.470195	61.81
No.146458	30.20	No.187320	58.64	No.255939	18.84	No.278642	45.88	No.472710	51.26
No.146625	73.23	No.187729	54.34	No.256811	29.84	No.284912	62.07	No.473771	85.03
No.146981	52.51	No.187867	57.86	No.258644	44.27	No.287446	66.18	No.473798	42.09
No.147399	52.57	No.188386	66.24	No.260271	52.74	No.287738	57.82	No.474599	79.39
No.147526	46.05	No.188526	65.61	No.260544	81.90	No.288864	53.61	No.477382	52.49
No.148798	63.49	No.188544	71.91	No.260808	72.25	No.289293	48.55	No.484140	81.88
No.148934	39.19	No.188629	57.46	No.261296	18.00	No.290475	50.20	No.492284	90.14
No.149137	48.26	No.188653	51.83	No.261340	51.95	No.291105	65.79	No.493841	69.13
No.149812	50.79	No.189301	51.08	No.261460	75.64	No.292011	40.21	No.500038	72.15
No.149954	35.12	No.189474	88.87	No.261541	27.34	No.293253	43.08	No.501026	71.56
No.151033	56.30	No.189640	82.40	No.261704	45.05	No.293813	50.55	No.502247	63.79
No.156930	67.18	No.190705	78.84	No.261928	59.40	No.294080	59.90	No.515263	65.13
No.157551	84.73	No.191294	89.56	No.261995	17.83	No.294295	62.45	No.517114	57.89
No.157995	45.27	No.192604	32.60	No.262202	39.97	No.295012	34.42	No.521025	62.76
No.161418	53.37	No.192937	19.22	No.262623	39.76	No.298163	60.39	No.521723	58.64
No.163131	46.39	No.193261	25.35	No.262684	25.39	No.299604	68.90	No.522540	74.24
No.164632	69.73	No.193268	35.56	No.262748	43.59	No.301862	48.50	No.523587	69.25
No.164935	60.08	No.194255	36.25	No.262756	49.53	No.301949	54.67	No.528892	73.49
No.165073	42.52 ###	No.194433	77.46	No.262819	41.67	No.303253	53.55	No.532171	69.57
No.165360	58.88	No.194936	97.60	No.263342	39.83	No.317128	69.80	No.532804	60.00
No.165910	55.01	No.195218	85.39	No.264044	35.43	No.339696	55.94	No.534592	69.62
No.166441	59.79	No.195577	52.49	No.264728	34.64	No.340818	52.17	No.537866	62.81
No.168198	84.85	No.195702	37.37	No.264785	80.62	No.343008	62.98	No.538245	69.60
No.169195	53.83	No.195747	50.57	No.265415	75.79	No.343133	48.31	No.540706	69.88
No.169780	56.32	No.195831	99.10	No.265721	51.29	No.344500	48.25	No.547640	60.33
No.170226	49.74	No.196041	79.83	No.265814	17.69	No.345102	76.36	No.548586	57.69
No.170544	66.23	No.196279	42.02	No.266126	60.45	No.347006	53.11	No.548656	65.56
No.170704	50.84	No.196462	82.72	No.266622	31.01	No.350815	53.89	No.550212	80.04
No.170940	39.11	No.196985	67.67	No.266837	32.24	No.351095	62.03	Adiponectin	100.00

Phosphorylation of AMPK normalized to the amount of AMPK in C2C12 myotubes treated for 5 min with 15 μg ml^{-1} adiponectin or the indicated small-molecule compounds (10 μM) (% relative to adiponectin). #, AdipoRon; ##, no.112254; ###, no.165073.

Extended Data Table 2 | Phosphorylation of AMPK in AdipoR knock-down C2C12 myotubes

	pAMPK/AMPK (ratio)	
Compounds	unrelated siRNA	AdipoR1 siRNA
Control	1.00	0.96
No.101962	5.35	5.10
No.103694	4.67	3.34
No.108049	4.75	2.68
No.112254	3.70	2.07
No.165073	1.29	1.23
No.168198	4.53	2.97
No.171723	2.13	2.39
No.171819	1.56	1.81
No.181432	2.03	2.40
No.182368	2.69	3.00
No.183665	2.88	2.83
No.189474	2.00	1.62
No.189640	1.85	1.82
No.191294	3.25	3.54
No.194936	2.11	2.49
No.195218	1.75	2.00
No.195831	2.88	2.98
No.196462	2.06	2.58
No.197248	2.09	2.55
No.197372	1.78	1.96
No.198637	2.24	2.51
No.200737	2.13	2.68
No.206685	1.76	2.39
No.209705	1.52	1.81
No.211156	2.36	2.59
No.214617	2.21	2.78
No.251327	2.85	3.15
No.260544	3.79	4.12
No.264785	3.70	3.58
No.268508	2.58	2.87
No.268949	3.10	2.82
No.272299	2.83	2.60
No.272350	2.03	2.54
No.274971	2.38	2.51
No.466151	2.22	1.94
No.473771	1.67	2.39
No.484140	2.34	2.30
No.492284	2.05	1.88
No.550212	1.91	2.14
Adiponectin	5.48	1.94

Phosphorylation of AMPK normalized to the amount of AMPK in C2C12 myotubes and transfected with or without the indicated siRNA duplex, treated for 5 min with adiponectin or the indicated small molecule.

Available online at www.sciencedirect.com

Metabolism

www.metabolismjournal.com

Basic Science

Dipeptidyl peptidase-4 inhibitor anagliptin ameliorates diabetes in mice with haploinsufficiency of glucokinase on a high-fat diet

Keizo Nakaya[a], *Naoto Kubota*[a,b,c,*], *Iseki Takamoto*[a], *Tetsuya Kubota*[a,c,d], *Hisayuki Katsuyama*[a], *Hiroyuki Sato*[a], *Kumpei Tokuyama*[e], *Shinji Hashimoto*[f], *Moritaka Goto*[f], *Takahito Jomori*[f], *Kohjiro Ueki*[a,b], *Takashi Kadowaki*[a,b,*]

[a] *Department of Diabetes and Metabolic Diseases, Graduate School of Medicine, University of Tokyo, Tokyo, Japan*
[b] *Translational Systems Biology and Medicine Initiative (TSBMI) University of Tokyo, Tokyo, Japan*
[c] *Division of Applied Nutrition, National Institute of Health and Nutrition, Tokyo, Japan*
[d] *Division of Cardiovascular Medicine, Toho University, Ohashi Hospital, Tokyo, Japan*
[e] *Graduate School of Comprehensive Human Sciences, University of Tsukuba, Tsukuba, Japan*
[f] *Mie Research Laboratories, Sanwa Kagaku Kenkyusho Co., Ltd., Mie, Japan*

ARTICLE INFO

Article history:
Received 7 October 2012
Accepted 10 January 2013

Keywords:
DPP-4 inhibitor
GLP-1
OGTT
Type 2 diabetes
β-cell mass

ABSTRACT

Objective. Type 2 diabetes is a chronic metabolic disorder characterized by hyperglycemia with insulin resistance and impaired insulin secretion. DPP-4 inhibitors have attracted attention as a new class of anti-diabetic agents for the treatment of type 2 diabetes. We investigated the effects of anagliptin, a highly selective DPP-4 inhibitor, on insulin secretion and insulin resistance in high-fat diet-fed mice with haploinsufficiency of glucokinase (GckKO) as animal models of type 2 diabetes.

Materials/Methods. Wild-type and GckKO mice were administered two doses of anagliptin by dietary admixture (0.05% and 0.3%) for 10 weeks.

Results. Both doses of anagliptin significantly inhibited the plasma DPP-4 activity and increased the plasma active GLP-1 levels in both the wild-type and GckKO mice to a similar degree. After 10 weeks of treatment with 0.3% anagliptin, body weight gain and food intake were significantly suppressed in both wild-type and GckKO mice. In addition, 0.3% anagliptin ameliorated insulin resistance and glucose intolerance in both genotypes of mice. On the other hand, treatment with 0.05% anagliptin was not associated with any significant change of the body weight, food intake or insulin sensitivity in either genotype of mice, but it did improve the glucose tolerance by enhancing insulin secretion and increasing the β-cell mass in both genotypes of mice.

Abbreviations: DPP-4, dipeptidyl peptidase-4; GLP-1, glucagon-like peptide-1; IRS-2, insulin receptor substrate-2; CREB, cAMP response element-binding protein; Gck, glucokinase; GIR, glucose infusion rate(s); EGP, endogenous glucose production; R_d, rate of glucose disappearance; ITT, insulin tolerance test; OGTT, oral glucose tolerance test.

* *Corresponding authors.* N. Kubota, is to be contacted at: Tel.: +81 3 5800 8818; fax: +81 3 5689 7209; T. Kadowaki Tel.: +81 3 5800 8815; fax: +81 3 5800 9797.
E-mail addresses: nkubota-tky@umin.ac.jp (N. Kubota), kadowaki-3im@h.u-tokyo.ac.jp (T. Kadowaki).

http://dx.doi.org/10.1016/j.metabol.2013.01.010

Conclusions. High-dose anagliptin treatment improved glucose tolerance by suppression of body weight gain and amelioration of insulin resistance, whereas low-dose anagliptin treatment improved glucose tolerance by enhancing insulin secretion.

1. Introduction

Type 2 diabetes is a chronic metabolic disorder characterized by hyperglycemia with insulin resistance and impaired insulin secretion. Progression to type 2 diabetes is influenced by genetic and environmental or acquired factors, such as a sedentary lifestyle and dietary habits that promote obesity. Most patients with type 2 diabetes are obese, and obesity is associated with insulin resistance. β-cell mass in adults exhibits plasticity, and adjustments in β-cell growth and survival maintain the balance between insulin supply and the metabolic demand. For example, obese individuals who do not develop diabetes exhibit an increase of the β-cell mass that appears to compensate for the increased metabolic load and obesity-associated insulin resistance. However, this β-cell adaptation eventually fails in the subset of obese individuals who develop type 2 diabetes [1–3]. In fact, most individuals with type 2 diabetes show a net decrease of the β-cell mass [1,4,5]. Thus, type 2 diabetes is a disease of relative insulin deficiency.

Glucagon-like peptide-1 (GLP-1), which is a gut-derived incretin hormone, stimulates glucose-dependent insulin secretion via the cAMP/PKA pathway. In addition, GLP-1 exerts multiple actions, including decrease of the body weight through suppression of appetite, stimulation of β-cell proliferation, and inhibition of β-cell apoptosis [6]. However, GLP-1 is rapidly converted to a bioinactive form by dipeptidyl peptidase-4 (DPP-4), the key enzyme responsible for cleaving and inactivating at the penultimate alanine residue [7–9]. Thus, DPP-4 inhibitors to block the enzymatic inactivation of GLP-1 have emerged as a new class of anti-diabetic agents for the treatment of type 2 diabetes.

Glucokinase (Gck) is the key rate-limiting enzyme in glucose metabolism in the β-cells. Gck catalyzes the conversion of glucose to glucose 6-phosphate, which is a critical process in glucose sensing for insulin secretion by the pancreatic β-cells. It has been shown that maturity-onset diabetes of the young type 2 (MODY2) can be caused by mutation in a single Gck gene allele [10,11]. Moreover, in type 2 diabetes, the mRNA expression and activity of Gck are significantly reduced, which is associated with impaired glucose-stimulated insulin release [12,13]. Mice with haploinsufficiency of Gck (GckKO mice) also exhibit glucose intolerance associated with a reduction in the insulin secretion in response to glucose [14]. In addition, GckKO mice show insufficient β-cell growth in response to high-fat diet-induced obesity-linked insulin resistance, leading to the development of diabetes [15]. Thus, GckKO mice fed a high-fat diet are considered as a useful animal model of diabetes, which show a time course of the disease similar to that seen in patients with type 2 diabetes.

In the present study, we investigated whether anagliptin, a highly selective DPP-4 inhibitor, might ameliorate glucose intolerance in high-fat diet-fed GckKO mice. Treatment with 0.3% anagliptin ameliorated the insulin resistance by suppression of body weight gain, which resulted in a decrease of the fasting plasma glucose and improvement of the glucose tolerance. On the other hand, treatment with 0.05% anagliptin improved glucose tolerance by enhancing insulin secretion, which was attributed to an increase of the β-cell mass, but did not suppress the body weight gain or ameliorate the insulin resistance. Taken together, both low and high doses of anagliptin improved glucose tolerance in the high-fat diet-fed GckKO diabetic mice. These findings suggest that anagliptin could be a potentially efficacious agent for the treatment of type 2 diabetic patients.

2. Materials and methods

2.1. Animals and genotyping

GckKO mice were generated as described previously [14]. Then, the original GckKO mice were back-crossed more than seven times with the C57BL/6 mice. The mice were housed under a 12-h light/dark cycle and fed standard chow (CE-2; CLEA) until 8 weeks of age and then allocated to either an HF diet alone or an HF diet containing a DPP-4 inhibitor. All of the experiments in this study were conducted on 8-week-old male littermates. The animal care and experimental procedures were approved by the Animal Care Committee of the University of Tokyo.

2.2. DPP-4 inhibitor treatment study

The composition of the HF diet (High Fat Diet 32; Clea Japan) was as described previously [15]. DPP-4 inhibitor was admixed with the HF diet at 0.05% or 0.3% (wt/wt). The DPP-4 inhibitor used in this study was anagliptin [16], prepared by Sanwa Kagaku Kenkyusho, Ltd.

2.3. Measurement of the plasma DPP-4 activity

Plasma DPP-4 activity was measured using a fluorometric assay with Gly-Pro-MCA (Peptide Institute, Osaka, Japan), modified from a previously published method [17]. In brief, 10 μL of a plasma sample was mixed with 90 μL of the reaction buffer (0.2 mmol/L Gly-Pro-MCA, 0.1 mg/mL BSA, 25 mol/L HEPES, 140 mol/L NaCl, pH 7.8). The mixture was incubated for 20 min at room temperature in the dark, and the reaction was stopped by the addition of 100 μL of 25% acetic acid. The fluorescence intensity of the liberated 7-amino-4-methylcoumarin (AMC) was measured with a 96-well plate fluorometer (1420 ARVOsx, PerkinElmer) at an excitation wavelength of 390 nm and emission wavelength of 460 nm. Plasma DPP-4 activity was calculated as nmol AMC/min/mL plasma, and the result in the treated samples was expressed as a percentage of that in the control.

2.4. Measurement of the plasma parameters

Plasma adiponectin levels were determined with a mouse adiponectin enzyme-linked immunosorbent assay kit (Otsuka

Pharmaceutical). Plasma leptin levels were determined with a mouse leptin ELISA kit (Morinaga Institute of Biological Science). Plasma levels of active GLP-1 were assayed with a Glucagon-Like Peptide-1 (Active) ELISA kit (Millipore).

2.5. *Insulin tolerance test*

Mice were given free access to food and then fasted during the study. They were intraperitoneally challenged with human insulin at 0.75 mU/g body weight (Humulin R), and venous blood samples were drawn at different time-points [18].

2.6. *Hyperinsulinemic–euglycemic clamp study*

Clamp studies were carried out as described previously [19], with slight modifications. In brief, 2 days before the study, an infusion catheter was inserted into the right jugular vein of the study animals under general anesthesia induced by sodium pentobarbital. Studies were performed on the mice under conscious and unstressed conditions after 6 h of fasting. A primed continuous infusion of insulin (Humulin R) was administered (7.5 mU/kg/min), and the blood glucose concentration, monitored every 5 min, was maintained at 100–130 mg/dL by administration of glucose (5 g of glucose/10 mL enriched to ~20% with [6,6-$^2H_2$]glucose (Sigma)) for 120 min. Blood was sampled via tail-tip bleeds at 90, 105 and 120 min for determination of the rate of glucose disappearance (*Rd*). *Rd* was calculated according to nonsteady-state equations, and endogenous glucose production was calculated as the difference between the *Rd* and the exogenous glucose infusion rate [19].

2.7. *Glucose tolerance test*

Mice were fasted for a sufficient period of time before the study, to eliminate the acute effects of anagliptin on glucose-stimulated insulin secretion and then orally loaded with glucose at 1.5 mg/g body weight. Blood samples were collected from the orbital sinus at different time-points, and the blood glucose was measured with an automatic glucometer (Glutest Ace, Sanwa Kagaku Kenkyusho) or the glucose CII-test Wako (Wako). Whole blood was collected and centrifuged in heparinized tubes, and the plasma samples were stored at −20 °C. Insulin levels were determined with an AlphaLISA insulin kit (PerkinElmer).

2.8. *Histological and immunohistochemical analysis of the islets*

Isolated pancreata were fixed with 4% paraformaldehyde at 4 °C overnight. Tissues were routinely processed for paraffin embedding, and 4-μm sections were cut and mounted on silanized slides. Pancreatic sections were stained with polyclonal guinea pig anti-swine insulin antibodies (diluted 1:100; DAKO). Images of the pancreatic tissue and islet β-cells were viewed on the monitor of a computer through a microscope connected to a camera with a charged-coupled device (Keyence). The areas of the pancreata and beta cells were traced manually and analyzed with WinROOF software (Mitani), as previously described [20]. The β-cell mass was calculated as the β-cell area, as assessed by immunostaining, relative to the area of the whole pancreas. More than 100 islets were analyzed per mouse in each group. BrdU incorporation was analyzed as described previously [15]. In brief, BrdU (100 mg/kg in saline; Sigma) was injected intraperitoneally, and the pancreas was removed 6 h later. The sections were immunostained with BrdU labeling and detection kit II (Roche Diagnostics). BrdU-positive beta cells were quantitatively assessed as a percentage of the total number of beta cells. Apoptotic cells were also detected in deparaffinized pancreatic sections using an in situ cell death detection kit (Roche Diagnostics), in accordance with the manufacturer's recommendations.

2.9. *Immunoblotting*

Polyclonal anti-IRS-2 antibody was purchased from Upstate. Antibodies to phospho-CREB and phospho-Akt were purchased from Cell Signaling Technology. The islets were sonicated in ice-cold buffer A (25 mol/L Tris–HCl, pH 7.4, 10 mol/L Na_3VO_4, 10 mol/L NaPPi, 100 mol/L NaF, 10 mol/L EDTA, 10 mol/L EGTA, and 1 mol/L phenylmethylsulfonyl fluoride) with an ultrasonic sonicator. Samples were separated by SDS-polyacrylamide gel electrophoresis, and immunodetection was performed with an ECL kit (Amersham Biosciences). Protein was prepared from more than 100 islets pooled from several mice of identical genotype, and 15 μg samples of the proteins were applied to the gel.

3. Results

3.1. *Treatment with 0.3% anagliptin decreased body weight gain and food intake*

After 10 weeks of treatment, 0.3% anagliptin significantly inhibited the plasma DPP-4 activity by more than 80%, and significantly increased the plasma levels of ad libitum active GLP-1 in the wild-type mice (Fig. 1A); 0.3% anagliptin also significantly inhibited the plasma DPP-4 activity and increased the plasma levels of ad libitum active GLP-1 in the GckKO mice, to degrees equivalent to those seen in the wild-type mice (Fig. 1B). Treatment with 0.3% anagliptin significantly decreased the body weight gain and food intake in the wild-type mice (Fig. 1, C and D), and also in the GckKO mice (Fig. 1, E and F). In contrast, this treatment had no significant effect on the rectal temperature or UCP-1 expression levels in the BAT in either mouse genotype (Fig. 1, G and H). Treatment with 0.3% anagliptin significantly decreased the weights of the epididymal fat and liver in the wild-type mice, and to an equivalent degree in the GckKO mice (Fig. 1, I and J). Furthermore, 0.3% anagliptin treatment significantly decreased the plasma leptin levels and significantly increased the plasma adiponectin levels in both the wild-type and GckKO mice (Fig. 1, K and L). These findings indicate that 0.3% anagliptin decreased body weight gain through inducing a reduction of the food intake in both wild-type and GckKO mice.

3.2. *Treatment with 0.3% anagliptin improved insulin resistance and glucose tolerance in wild-type and GckKO mice*

The insulin tolerance test (ITT) revealed that the glucose-lowering effect of insulin was significantly increased in the

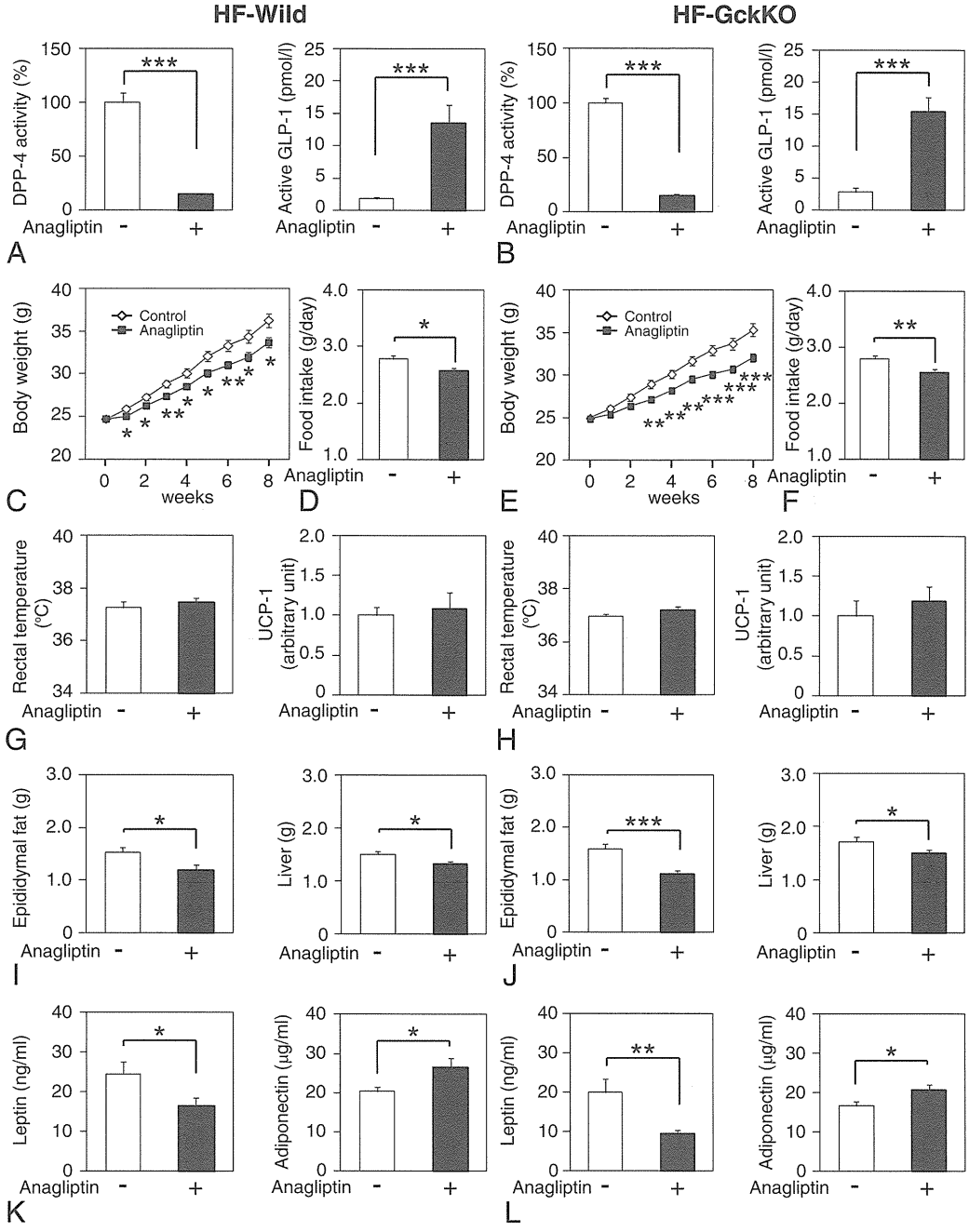

Fig. 1 – Treatment with 0.3% anagliptin decreased body weight gain and food intake. A and B, DPP-4 activities (left panels) and active GLP-1 levels (right panels) in wild-type (A) and GckKO (B) mice not treated (open bars) or treated (closed bars) with anagliptin (n=11–12). C and D, body weights (left panel, n=30) and food intake (right panel, n=11–12) in wild-type mice not treated (open diamonds and open bar) or treated (closed squares and closed bar) with anagliptin. E and F, body weights (left panel, n=23–24) and food intake (right panel, n=11–12) of GckKO mice not treated (open diamonds and open bar) or treated (closed squares and closed bar) with anagliptin. G and H, rectal temperature (left panels, n=23–24) and UCP-1 expression levels (right panels, n=5–6) in wild-type (G) and GckKO (H) mice not treated (open bars) or treated (closed bars) with anagliptin. I and J, weights of epididymal fat (left panels) and liver (right panels) in wild-type (I) and GckKO (J) mice not treated (open bars) or treated (closed bars) with anagliptin (n=22–24). K and L, leptin (left panels) and adiponectin (right panels) levels in wild-type (K) and GckKO (L) mice not treated (open bars) or treated (closed bars) with anagliptin (n=12–14).Values are means±S.E. of data obtained from the analysis of wild-type and GckKO mice. *, p<0.05. **, p<0.01. ***, p<0.001.

0.3% anagliptin-treated wild-type mice as compared with that in the untreated wild-type mice (Fig. 2A). Although the GckKO mice showed hyperglycemia in the fed state before insulin administration as compared with the wild-type mice, the glucose-lowering effect of insulin was also significantly more pronounced in the 0.3% anagliptin-

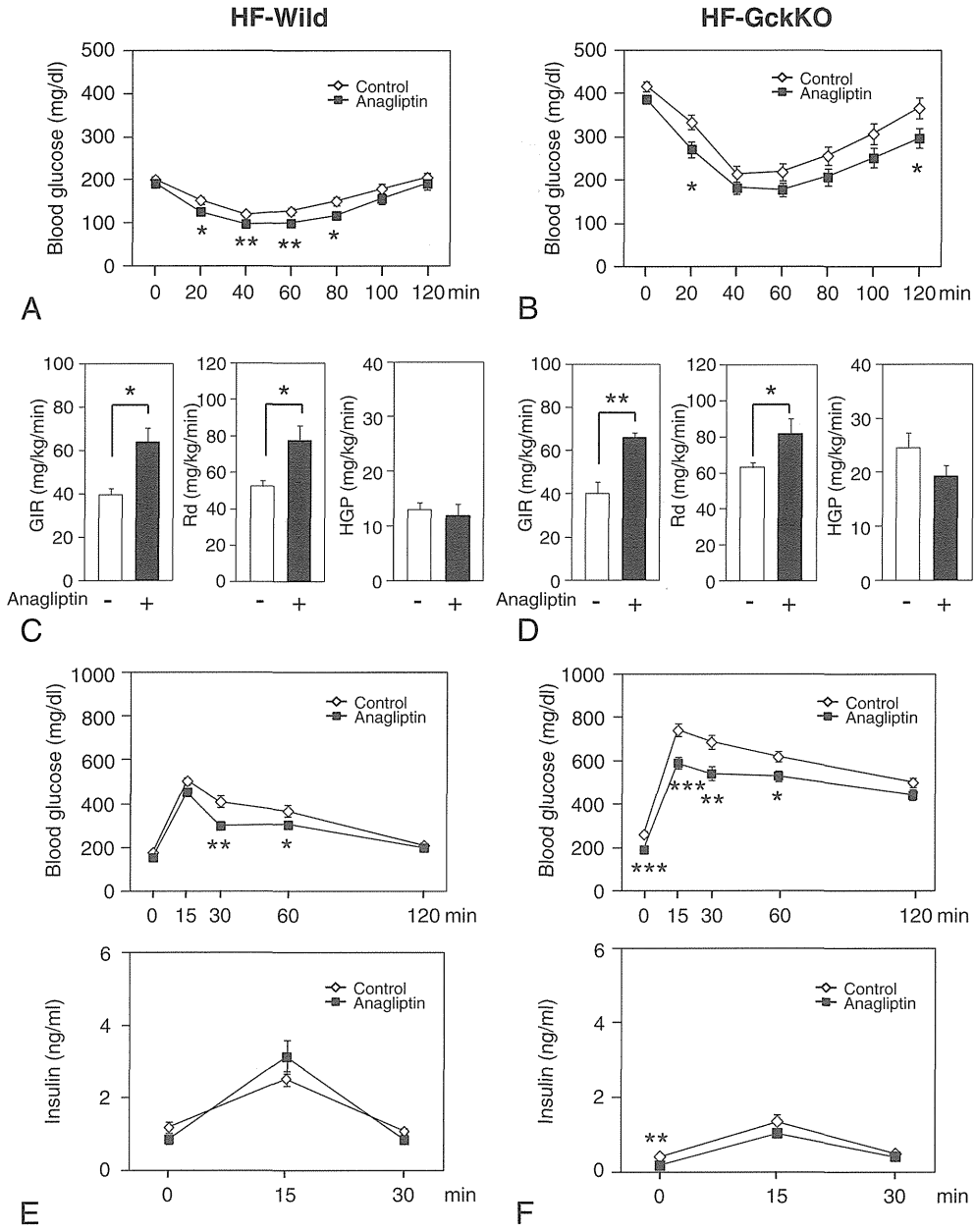

Fig. 2 – Treatment with 0.3% anagliptin improved insulin resistance and glucose tolerance in the wild-type and GckKO mice. A and B, blood glucose levels during the ITT in wild-type (A) and GckKO (B) mice not treated (open diamonds) or treated (closed squares) with anagliptin (n=30). C and D, GIR (left panels), Rd (middle panels) and HGP (right panels) in wild-type (C) and GckKO (D) mice not treated (open bars) or treated (closed bars) with anagliptin (n=5–6). E and F, blood glucose (upper panels) and plasma insulin (bottom panels) levels during OGTT in wild-type (E) and GckKO (F) mice not treated (open diamonds) or treated (closed squares) with anagliptin (n=23–24). Values are means±S.E. of data obtained from the analysis of wild-type and GckKO mice. *, $p<0.05$. **, $p<0.01$. ***, $p<0.001$.

treated GckKO mice as compared with that in the untreated GckKO mice (Fig. 2, A and B). Consistent with the results of the ITT, the glucose infusion rate (GIR) and rate of glucose disappearance (Rd) were significantly increased after 0.3% anagliptin treatment in both the wild-type and GckKO mice (Fig. 2, C and D). In contrast, the treatment had no effect on the endogenous glucose production (HGP) in either genotype of mice (Fig. 2, C and D). Blood glucose levels before and after glucose loading were significantly higher in the untreated GckKO mice than in the untreated wild-type mice, along with impaired insulin secretion, as we previously reported (Fig. 2, E and F) [15]. In an oral glucose tolerance test (OGTT), the blood glucose levels at 30 min and 60 min after glucose loading were significantly lower in the 0.3% anagliptin-treated wild-type mice than in the untreated wild-type mice (Fig. 2E). The blood glucose levels in 0.3% anagliptin-treated GckKO mice before and after glucose loading were also

significantly lower than those in untreated GckKO mice (Fig. 2F). On the other hand, no significant increment of insulin secretion by anagliptin was observed in either genotype of mice (Fig. 2, E and F). These findings suggest that 0.3% anagliptin improves glucose tolerance predominantly by ameliorating insulin resistance rather than by increasing insulin secretion.

3.3. *No increment of β-cell mass was observed following 0.3% anagliptin treatment in either genotype of mice*

The β-cell mass tended to be lower in the untreated GckKO mice as compared with that in the untreated wild-type mice ($P=0.06$) (Fig. 3, A, B, E and F). The percentage of cells incorporating BrdU was significantly lower in the untreated GckKO mice than in the untreated wild-type mice ($P<0.01$) (Fig. 3, C and G). In contrast, the percentage of TUNEL-positive cells tended to be higher in the untreated GckKO mice than in the untreated wild-type mice ($P=0.12$) (Fig. 3, D and H). After 10 weeks of treatment with 0.3% anagliptin, the β-cell mass was indistinguishable from that in the untreated mice in both genotypes of mice (Fig. 3, A, B, E and F). Moreover, treatment with 0.3% anagliptin did not have any significant effect on the percentage of cells incorporating BrdU or the number of TUNEL-positive cells among the β-cells in either genotype of mice (Fig. 3, C, D, G and H).

3.4. *Treatment with 0.05% anagliptin had no effect on the body weight or insulin sensitivity, but improved glucose tolerance by increasing insulin secretion*

It was considered that the absence of any effect of 0.3% anagliptin on the β-cell mass was attributable to its effect of suppressing body weight gain and ameliorating insulin resistance. Therefore, we next investigated the dose-dependent effects of anagliptin on the active GLP-1 levels, the body weight, insulin resistance and glucose tolerance in wild-type mice. The active GLP-1 levels were significantly increased, in a dose-dependent manner, after anagliptin treatment (Fig. 4A). After 8 weeks of treatment, the body weight gain was indistinguishable between the untreated and 0.05% anagliptin-treated mice (Fig. 4B). In contrast, treatment with 0.3% anagliptin was associated with a significant reduction of the body weight gain (Fig. 4B) as seen in Fig. 1C. In the ITT, although the blood glucose levels after insulin administration were indistinguishable between untreated mice and the mice treated with 0.05% anagliptin, the blood glucose levels before and after insulin administration were significantly decreased in the 0.3% anagliptin-treated mice as compared with those in the untreated mice (Fig. 4C). In the OGTT, the blood glucose levels after glucose loading were significantly decreased, along with increased insulin secretion, in the 0.05% anagliptin-treated mice (Fig. 4D). On the other hand, whereas the blood

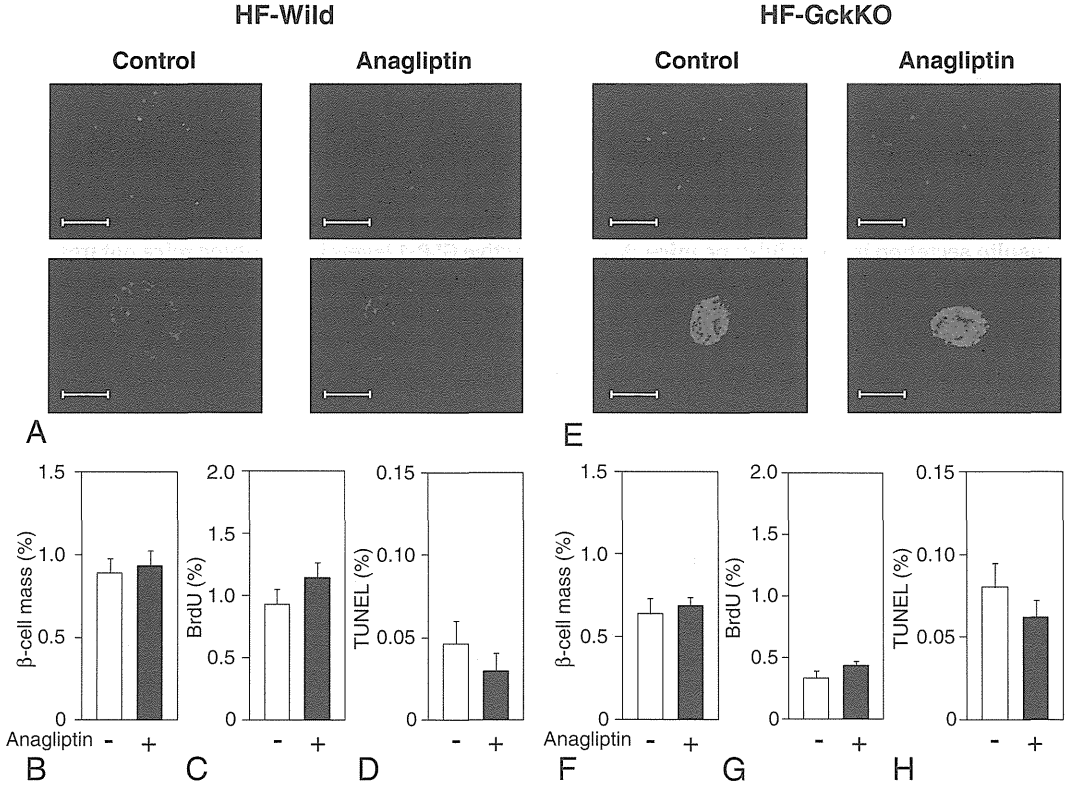

Fig. 3 – Effect of 0.3% anagliptin on the β-cell mass. Histological analysis of pancreatic β-cells (A and E) (upper panels; scale bar = 1000 μm, lower panels; scale bar = 100 μm), quantitation of β-cell mass (B and F), BrdU incorporation (C and G) and TUNEL staining (D and H) in wild-type (A–D) and GckKO (E–H) mice not treated (open bars) or treated (closed bars) with anagliptin (n = 6–9). Sections were stained with anti-insulin antibody. Values are means ± S.E. of data obtained from the analysis of wild-type and GckKO mice.

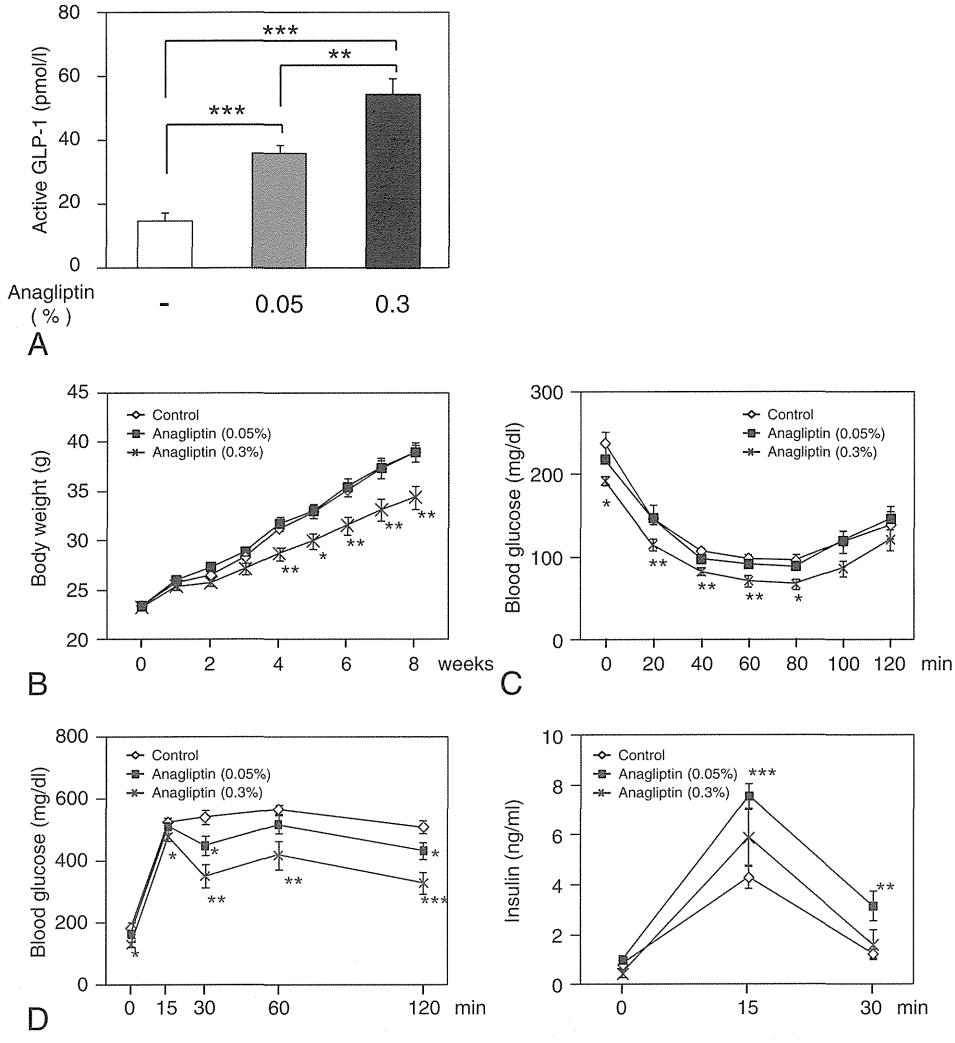

Fig. 4 – Treatment with 0.05% anagliptin had no effect on the body weight or insulin sensitivity, but improved glucose tolerance by increasing insulin secretion in the wild-type mice. A, plasma active GLP-1 levels in wild-type mice not treated (open bars) or treated (0.05%: gray bars, 0.3%: closed bars) with anagliptin. B, body weights of wild-type mice not treated (open diamonds) or treated (0.05%: closed squares and 0.3%: cross-lines) with anagliptin. C, blood glucose levels during the ITT in wild-type mice not treated (open diamonds) or treated (0.05%: closed squares and 0.3%: cross-lines) with anagliptin. D, blood glucose (left panel) and plasma insulin (right panel) levels during OGTT in wild-type mice not treated (open diamonds) or treated (0.05%: closed squares and 0.3%: cross-lines) with anagliptin (n=8). Values are means±S.E. of data obtained from the analysis of wild-type mice. *, $p<0.05$. **, $p<0.01$. ***, $p<0.001$.

glucose levels before and after glucose loading were significantly lower in the 0.3% anagliptin-treated mice than those in the untreated mice, the plasma levels of insulin before and after glucose loading were indistinguishable between untreated mice and the mice treated with 0.3% anagliptin (Fig. 4D). These results suggest that 0.05% anagliptin improved glucose tolerance by increasing insulin secretion, whereas 0.3% anagliptin improved glucose tolerance by ameliorating insulin resistance.

3.5. *0.05% anagliptin had no effect on the body weight or food intake of either wild-type or GckKO mice*

After 10 weeks of treatment, 0.05% anagliptin significantly inhibited the plasma DPP-4 activity by more than 70%, and significantly increased the plasma levels of ad libitum active GLP-1 in both the wild-type and GckKO mice (Fig. 5, A and B). Treatment with 0.05% anagliptin had little effect on the body weight gain or food intake in either the wild-type or the GckKO mice (Fig. 5, C, D, E and F). The rectal temperature and UCP-1 expression levels in the BAT were also indistinguishable between the untreated and 0.05% anagliptin-treated mice of either genotype (Fig. 5, G and H). Furthermore, treatment with 0.05% anagliptin also had no effect on the weights of epididymal fat or the liver in either genotype of mice (Fig. 5, I and J). The plasma leptin and adiponectin levels were indistinguishable between the untreated and 0.05% anagliptin-treated mice of either genotype (Fig. 5, K and L). These findings indicate that 0.05% anagliptin had no effect on the body weight or food intake in either the wild-type or the GckKO mice.

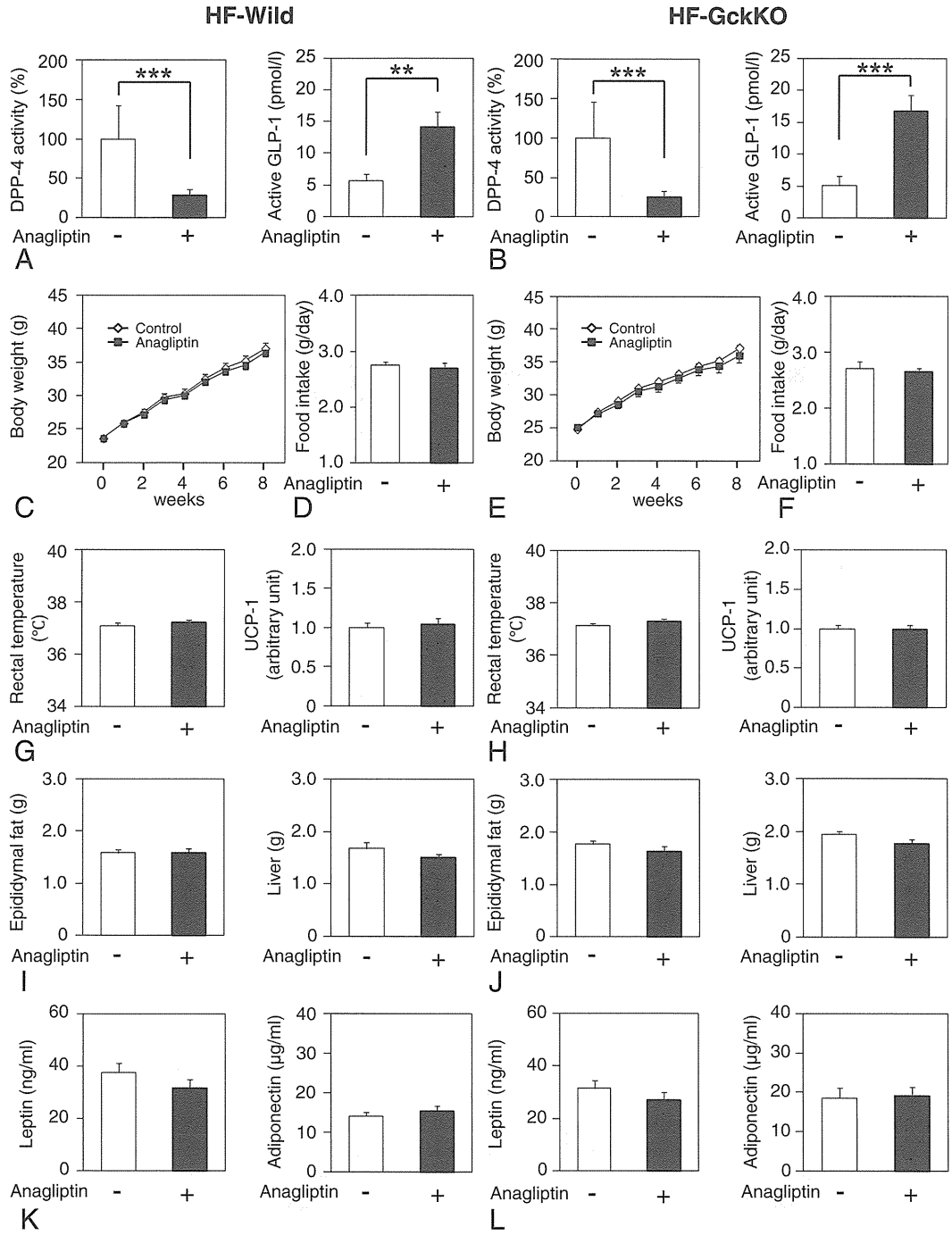

Fig. 5 – Treatment with 0.05% anagliptin had no effect on the body weight or food intake in either the wild-type or GckKO mice. A and B, DPP-4 activities (left panels) and active GLP-1 levels (right panels) in wild-type (A, n=15–16) and GckKO (B, n=11–12) mice not treated (open bars) or treated (closed bars) with anagliptin. C and D, body weights (left panel, n=21) and food intake (right panel, n=8) in wild-type mice not treated (open diamonds and open bar) or treated (closed squares and closed bar) with anagliptin. E and F, body weights (left panel, n=18–21) and food intake (right panel, n=10) in GckKO mice not treated (open diamonds and open bar) or treated (closed squares and closed bar) with anagliptin. G and H, rectal temperature (left panels, n=18–21) and UCP-1 expression levels (right panels, n=5–6) in wild-type (G) and GckKO (H) mice not treated (open bars) or treated (closed bars) with anagliptin. I and J, weights of epididymal fat (left panels) and liver (right panels) in wild-type (I) and GckKO (J) mice not treated (open bars) or treated (closed bars) with anagliptin (n=14–16). K and L, leptin (left panels) and adiponectin (right panels) levels in wild-type (K) and GckKO (L) mice not treated (open bars) or treated (closed bars) with anagliptin (n=14–16). Values are means±S.E. of data obtained from the analysis of wild-type and GckKO mice. **, p<0.01. ***, p<0.001.

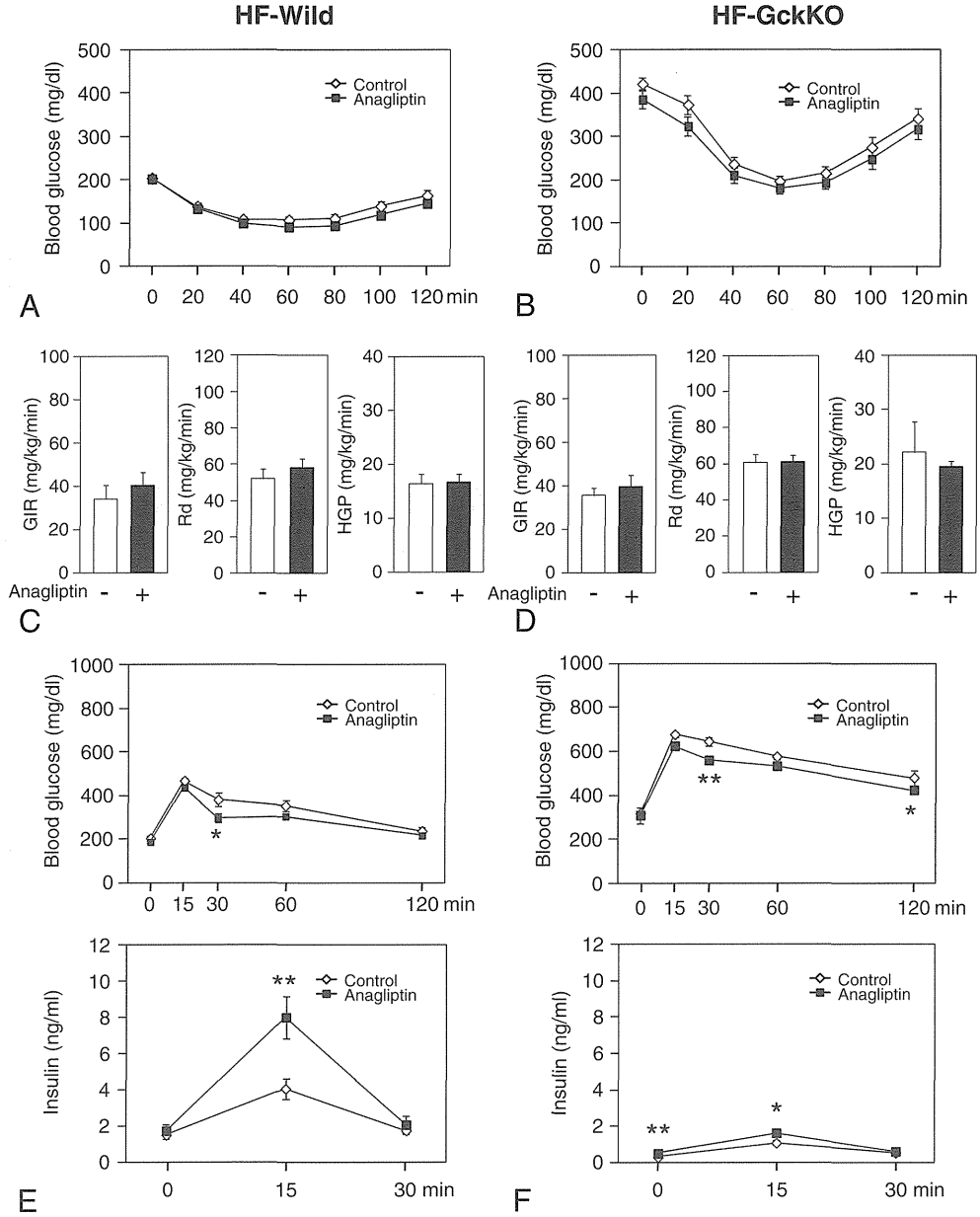

Fig. 6 – Treatment with 0.05% anagliptin improved glucose tolerance by increasing the insulin secretion in both wild-type and GckKO mice. A and B, blood glucose levels during the ITT in wild-type (A, n = 15–16) and GckKO (B, n = 18–21) mice not treated (open diamonds) or treated (closed squares) with anagliptin. C and D, GIR (left panels), Rd (middle panels) and HGP (right panels) in wild-type (C) and GckKO (D) mice not treated (open bars) or treated (closed bars) with anagliptin (n = 4). E and F, blood glucose (upper panels) and plasma insulin (bottom panels) levels during OGTT in wild-type (E, n = 12) and GckKO (F, n = 23–24) mice not treated (open diamonds) or treated (closed squares) with anagliptin. Values are means ± S.E. of data obtained from the analysis of wild-type and GckKO mice. *, $p < 0.05$. **, $p < 0.01$.

3.6. *0.05% anagliptin improved glucose tolerance by enhancing insulin secretion in both wild-type and GckKO mice*

Unlike 0.3% anagliptin treatment, the ITT showed that treatment with 0.05% anagliptin had no effect on the insulin sensitivity in the mice of either genotype (Fig. 6, A and B). Consistent with the results of the ITT, the GIR and Rd, as well as HGP, were indistinguishable between the untreated and 0.05% anagliptin-treated mice of either genotype (Fig. 6, C and D). These results indicate that the amelioration of insulin resistance by 0.3% anagliptin might be largely dependent on the suppression of body weight gain. In the OGTT, the blood glucose levels after glucose loading were significantly lower in the 0.05% anagliptin-treated wild-type mice than in the untreated wild-type mice, with increment of the insulin secretion (Fig. 6E). The blood glucose levels after glucose loading were also significantly lower in the anagliptin-treated GckKO mice than in the untreated GckKO mice (Fig. 6F). Treatment with 0.05% anagliptin significantly increased the

insulin secretion before and after glucose loading in the GckKO mice, unlike the case following treatment with 0.3% anagliptin (Fig. 6F). These data suggest that 0.05% anagliptin improved glucose tolerance with enhancement of insulin secretion in the GckKO mice as well as in the wild-type mice.

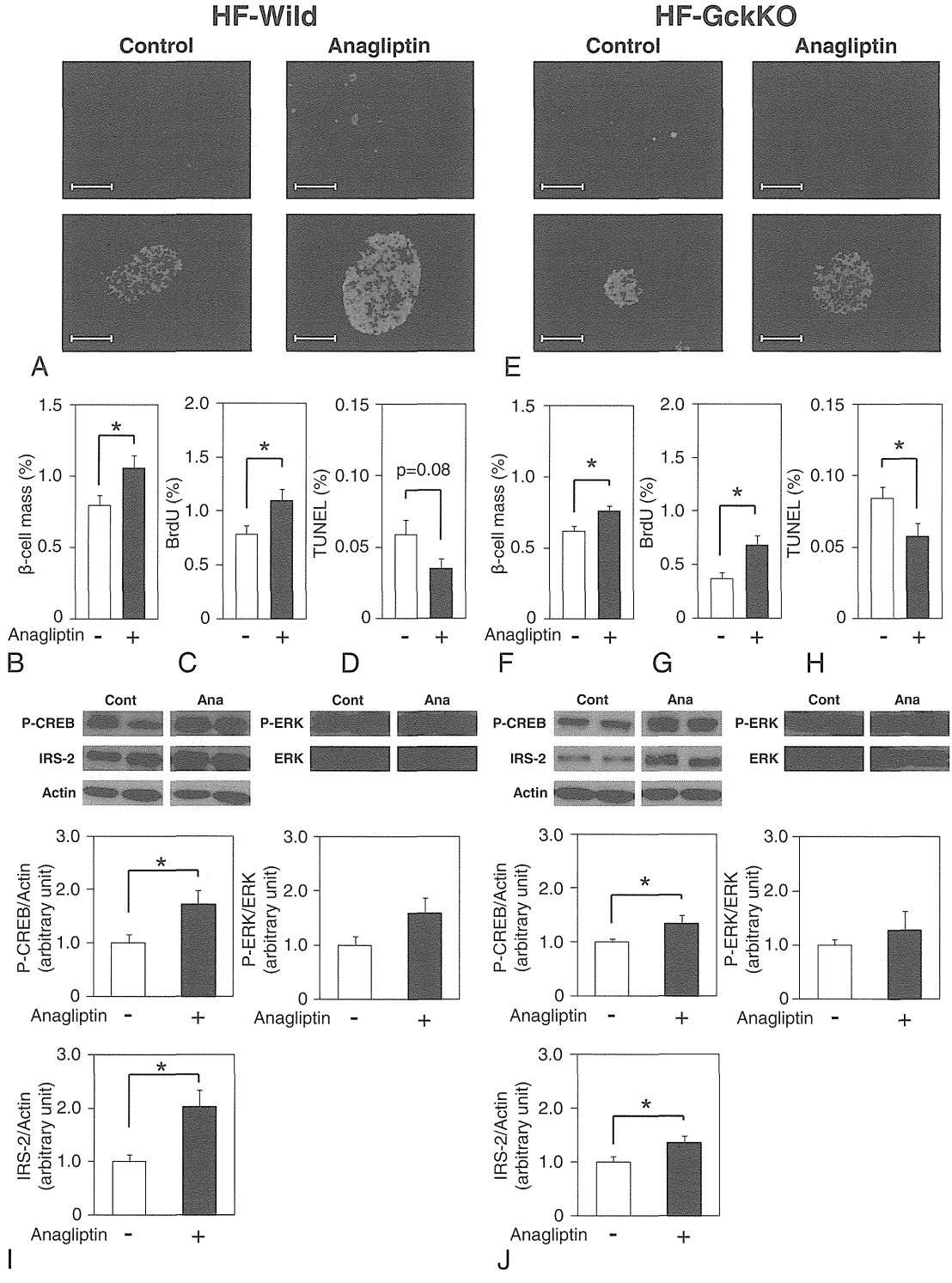

Fig. 7 – Treatment with 0.05% anagliptin increased the β-cell mass. Histological analysis of pancreatic β-cells (A and E) (upper panels; scale bar = 1000 μm, lower panels; scale bar = 100 μm), quantitation of β-cell mass (B and F), BrdU incorporation (C and G) and TUNEL staining (D and H) in wild-type (A–D) and GckKO (E–H) mice not treated (open bars) or treated (closed bars) with anagliptin (n = 8–10). Sections were stained with anti-insulin antibody. I and J, protein levels of IRS-2, and phosphorylation level of CREB and ERK in the islets in wild-type (I) and GckKO (J) mice not treated (open bars) or treated (closed bars) with anagliptin (n = 5–10). Values are means ± S.E. of data obtained from the analysis of wild-type and GckKO mice. *, $p < 0.05$.

3.7. *Treatment with 0.05% anagliptin increased the β-cell mass in both wild-type and GckKO mice*

We investigated the effects of 0.05% anagliptin on the β-cell mass in wild-type and GckKO mice, with no difference in the body weight or insulin sensitivity between the untreated and treated mice. After 10 weeks of treatment, 0.05% anagliptin significantly increased the β-cell mass in the wild-type mice (Fig. 7, A and B); the treatment also produced a slight, but significant increase of the β-cell mass in the GckKO mice (Fig. 7, E and F). However, the increment of β-cell mass tended to be lower in the GckKO mice than that of wild-type mice (0.26% in wild-type mice vs. 0.14% in GckKO mice) (Fig. 7, A, B, E and F), suggesting that the increment of β-cell mass by 0.05% anagliptin may be dependent, at least in part, on glucose metabolism via glucokinase. The percentage of cells incorporating BrdU was also significantly increased in both the 0.05% anagliptin-treated groups as compared with that in the untreated groups (Fig. 7, C and G). The percentage of TUNEL-positive cells tended to be decreased in the 0.05% anagliptin-treated wild-type mice as compared with that in the untreated wild-type mice, and the percentage of TUNEL-positive cells was significantly decreased in the 0.05% anagliptin-treated GckKO mice as compared with that in the untreated GckKO mice (Fig. 7, D and H). We next investigated phosphorylation of CREB and the protein level of IRS-2 in the islets of untreated and 0.05% anagliptin-treated mice. Phosphorylation of CREB and the protein level of IRS-2 were significantly increased in both the 0.05% anagliptin-treated groups as compared to the untreated groups (Fig. 7, I and J). However, the increment of CREB phosphorylation and up-regulation of IRS-2 tended to be less pronounced in the 0.05% anagliptin treated GckKO mice as compared with those in 0.05% anagliptin treated wild-type mice (CREB: 1.72%±0.07% in wild-type mice vs. 1.35%±0.14% in GckKO mice, IRS-2: 2.20%±0.10% in wild-type mice vs. 1.36%±0.12% in GckKO mice) (Fig. 7, I and J). On the other hand, the effect on ERK phosphorylation was not significantly different between the untreated and 0.05% anagliptin-treated mice of either genotype (Fig. 7, I and J).

4. Discussion

Decrease of the β-cell mass, as well as β-cell dysfunction and development of insulin resistance, has recently been reported to play crucial roles in the pathogenesis of type 2 diabetes [1,21]. In the present study, we investigated whether anagliptin might be capable of ameliorating insulin resistance and glucose intolerance in GckKO mice on a high-fat diet. High-dose (0.3%) anagliptin treatment decreased body weight gain via suppression of food intake, leading to improved glucose tolerance and amelioration of insulin resistance. On the other hand, low-dose (0.05%) anagliptin treatment, which had no apparent effect on the body weight or insulin sensitivity, improved glucose tolerance by enhancing insulin secretion and increasing the β-cell mass. These data suggest that high-dose anagliptin treatment improved glucose tolerance by suppression of body weight gain and amelioration of insulin resistance, whereas low-dose anagliptin treatment improved glucose tolerance by enhancing insulin secretion.

However, the anagliptin-treated GckKO mice still showed sustained hyperglycemia, although anagliptin increased the active GLP-1 level in the GckKO mice, to degrees equivalent to those seen in the wild-type mice. Incretin effects may be, at least in part, dependent on the glucose metabolism. In fact, the effect of GLP-1 analogue on insulin secretion in response to glucose was attenuated in GckKO islets compared with WT islets [22]. Thus, impairment of glucose metabolism by haploinsufficiency of glucokinase is considered to be decreased GLP-1-induced insulin secretion, which may be the reason why anagliptin does not prevent the onset and development of diabetes. Considering that glucose metabolism in the β-cells is progressively impaired in type 2 diabetes [12], DPP-4 inhibitors and GLP-1 analogues may be more effective in the treatment of early-stage type 2 diabetes, in which milder abnormalities of glucose metabolism may be expected.

It has been reported from preclinical studies that GLP-1 analogues and DPP-4 inhibitors increase the β-cell mass through their effects of increasing β-cell proliferation and inhibiting β-cell apoptosis [23–26]. Shirakawa et al. reported that desfluorositagliptin (DFS), DPP-4 inhibitor, protected against β-cell apoptosis and restored the β-cell mass in GckKO mice fed with a diet containing sucrose and linoleic acid [22]. Low-dose anagliptin treatment indeed increased β-cell mass through stimulation of β-cell proliferation and inhibition of β-cell apoptosis in GckKO mice on a high-fat diet. GLP-1 analogues have been shown to increase the cAMP levels in human islets and MIN6 cells, which promote IRS-2 expression and stimulate Akt phosphorylation [27,28]. Moreover, GLP-1 analogue has been shown to increase the β-cell mass in wild-type mice, but not in IRS-2 KO mice, suggesting that insulin signaling via IRS-2 is essential for the effects of the GLP-1 analogue on the β-cell mass to be expressed [27]. Consistent with these results, low-dose anagliptin treatment increased β-cell mass along with the enhancement of CREB phosphorylation and IRS-2 expression.

Besides the CREB/IRS-2 pathway, ERK phosphorylation via cAMP/PKA has also been reported to be stimulated by the GLP-1 analogues, leading to increased expression of CyclinD1 and increased proliferation in pancreatic β-cell lines [29,30]. In the present study, however, the ERK phosphorylation level (Fig. 7, I and J) and CyclinD1 expression (data not shown) were not significantly different between the anagliptin-treated and untreated islets in either genotype of mice, although BrdU incorporation was elevated in the anagliptin-treated mice. These discrepancies may be caused by the difference in the GLP-1 activity between GLP-1 analogues and DPP-4 inhibitors. In the case of experiment using GLP-1, Gomez et al. treated MIN6 cells with 10 nmol/L GLP-1 to investigate GLP-1-stimulated ERK phosphorylation [29]. On the other hand, GLP-1 levels following treatment with anagliptin and other DPP-4 inhibitors were ~10 pmol/L [31]. Moreover, in the experiment conducted using INS-1 cells, GLP-1 produced short-term stimulation of ERK phosphorylation [30], suggesting that the ERK pathway may be involved in the short-term regulation of β-cell growth, while the CREB/IRS-2 pathway may be involved in the long-term regulation of β-cell growth.

Why did high-dose anagliptin fail to increase the β-cell mass or glucose-stimulated insulin secretion although the active GLP-1 levels were significantly increased? Expansion of the pancreatic β-cell mass and increase in insulin secretion are known to occur for maintaining normal glucose levels in the event of development of insulin resistance [21,32]; on the other hand, β-cell growth and insulin secretion are suppressed with the amelioration of insulin resistance. In fact, Gedulin et al. have reported absence of any increase of the β-cell mass or fasting plasma insulin levels in GLP-1 analogue-treated Zucker rats, which showed suppressed body weight gain and improved insulin sensitivity [33]; it is likely that the ameliorating effect of high-dose anagliptin on insulin resistance with suppression of body weight gain may have led to the absence of increase of the β-cell mass and insulin secretion. Instead, the elevated active GLP-1 might have obscured the suppression of insulin secretion due to amelioration of insulin resistance. In fact, the fasting plasma insulin and glucose levels tended to remain low in the high-dose anagliptin-treated mice.

Although both GLP-1 analogues and DPP-4 inhibitors have been shown to improve several indices of β-cell function, these two classes of drugs exert different effects on the body weight and appetite [34]. The differential effects on the body weight and appetite may be explained by the greater concentration of GLP-1 achieved with GLP-1 analogue treatment than with DPP-4 inhibition. In a clinical study comparing exenatide and sitagliptin, the mean 2-h plasma exenatide concentration was 64 pmol/L in patients treated with exenatide as compared to the mean 2-h postprandial plasma GLP-1 concentration of 15 pmol/L in patients treated with sitagliptin (baseline GLP-1 concentration 7.2 pmol/L) [35]. Considering that the plasma GLP-1 concentration was higher in the mice treated with high-dose anagliptin than in the mice treated with low-dose anagliptin in this study, the possibility that the difference in the plasma GLP-1 concentration between the two groups may account for the differential effects on the body weight and appetite cannot be excluded. However, unlike the effects of the GLP-1 receptor analogues, the effects of DPP-4 inhibitors on the body weight and appetite were small or absent in clinical studies [34]. Considering these findings, the low-dose, rather than high-dose, anagliptin used in this study may be more clinically relevant in the treatment of type 2 diabetes.

In conclusion, both low and high doses of anagliptin improved glucose tolerance in the high-fat diet-fed GckKO diabetic mice. These findings suggest that anagliptin could be a potentially efficacious agent for the treatment of type 2 diabetic patients.

Author contributions

N.K. researched the data, wrote the manuscript, contributed to the discussion, and reviewed and edited the manuscript. I.T., T.K., H.K., H.S. and K.T. researched the data and contributed to the discussion. S.H. contributed to the discussion. M.G. researched the data and contributed to the discussion. T.J. and K.U. contributed to the discussion. T.K. reviewed and edited the manuscript, and contributed to the discussion.

Funding

This work was supported by a grant for TSBMI from the Ministry of Education, Culture, Sports, Science and Technology of Japan; a Grant-in-Aid for Scientific Research in Priority Areas (A) (16209030), (A) (18209033), and (S) (20229008) from the Ministry of Education, Culture, Sports, Science, and Technology of Japan (to T. Kadowaki); and a Grant-in-Aid for Scientific Research in Priority Areas (C) (19591037) and (B) (21390279) from the Ministry of Education, Culture, Sports, Science, and Technology of Japan (to N.Kubota).

Acknowledgment

We thank Tomoko Asano, Eriko Nozaki, Ayumi Nagano, Eishin Hirata, Kousuke Yokota, Yuko Okonogi, Miyoko Suzuki-Nakazawa, Masahiro Nakamaru, and Manami Takagi for their excellent technical assistance and assistance with the animal care.

Conflicts of interest

The authors report no conflicts of interest.

REFERENCES

[1] Butler AE, Janson J, Bonner-Weir S, Ritzel R, Rizza RA, Butler PC. Beta-cell deficit and increased beta-cell apoptosis in humans with type 2 diabetes. Diabetes 2003;52:102–10.
[2] Weir GC, Laybutt DR, Kaneto H, Bonner-Weir S, Sharma A. Beta-cell adaptation and decompensation during the progression of diabetes. Diabetes 2001;50(Suppl 1):S154–9.
[3] Dickson LM, Rhodes CJ. Pancreatic beta-cell growth and survival in the onset of type 2 diabetes: a role for protein kinase B in the Akt? Am J Physiol Endocrinol Metab 2004;287: E192–8.
[4] Sakuraba H, Mizukami H, Yagihashi N, Wada R, Hanyu C, Yagihashi S. Reduced beta-cell mass and expression of oxidative stress-related DNA damage in the islet of Japanese type II diabetic patients. Diabetologia 2002;45:85–96.
[5] Yoon KH, Ko SH, Cho JH, Lee JM, Ahn YB, Song KH, et al. Selective beta-cell loss and alpha-cell expansion in patients with type 2 diabetes mellitus in Korea. J Clin Endocrinol Metab 2003;88:2300–8.
[6] Baggio LL, Drucker DJ. Biology of incretins: GLP-1 and GIP. Gastroenterology 2007;132:2131–57.
[7] Mentlein R, Gallwitz B, Schmidt WE. Dipeptidyl-peptidase IV hydrolyses gastric inhibitory polypeptide, glucagon-like peptide-1(7–36)amide, peptide histidine methionine and is responsible for their degradation in human serum. Eur J Biochem 1993;214:829–35.
[8] Deacon CF, Johnsen AH, Holst JJ. Degradation of glucagon-like peptide-1 by human plasma in vitro yields an N-terminally truncated peptide that is a major endogenous metabolite in vivo. J Clin Endocrinol Metab 1995;80:952–7.
[9] Kieffer TJ, McIntosh CH, Pederson RA. Degradation of glucose-dependent insulinotropic polypeptide and truncated glucagon-like peptide 1 in vitro and in vivo by dipeptidyl peptidase IV. Endocrinology 1995;136:3585–96.

[10] Froguel P, Zouali H, Vionnet N, Velho G, Vaxillaire M, Sun F, et al. Familial hyperglycemia due to mutations in glucokinase. Definition of a subtype of diabetes mellitus. N Engl J Med 1993;328:697–702.
[11] Velho G, Blanche H, Vaxillaire M, Bellanne-Chantelot C, Pardini VC, Timsit J, et al. Identification of 14 new glucokinase mutations and description of the clinical profile of 42 MODY-2 families. Diabetologia 1997;40:217–24.
[12] Del Guerra S, Lupi R, Marselli L, Masini M, Bugliani M, Sbrana S, et al. Functional and molecular defects of pancreatic islets in human type 2 diabetes. Diabetes 2005;54:727–35.
[13] Bouche C, Serdy S, Kahn CR, Goldfine AB. The cellular fate of glucose and its relevance in type 2 diabetes. Endocr Rev 2004;25:807–30.
[14] Terauchi Y, Sakura H, Yasuda K, Iwamoto K, Takahashi N, Ito K, et al. Pancreatic beta-cell-specific targeted disruption of glucokinase gene. Diabetes mellitus due to defective insulin secretion to glucose. J Biol Chem 1995;270:30253–6.
[15] Terauchi Y, Takamoto I, Kubota N, Matsui J, Suzuki R, Komeda K, et al. Glucokinase and IRS-2 are required for compensatory beta cell hyperplasia in response to high-fat diet-induced insulin resistance. J Clin Invest 2007;117:246–57.
[16] Kato N, Oka M, Murase T, Yoshida M, Sakairi M, Yamashita S, et al. Discovery and pharmacological characterization of N-[2-({2-[(2S)-2-cyanopyrrolidin-1-yl]-2-oxoethyl}amino)-2-methylpropyl]-2-methyl pyrazolo[1,5-a]pyrimidine-6-carboxamide hydrochloride (anagliptin hydrochloride salt) as a potent and selective DPP-IV inhibitor. Bioorg Med Chem 2011;19:7221–7.
[17] Deacon CF, Hughes TE, Holst JJ. Dipeptidyl peptidase IV inhibition potentiates the insulinotropic effect of glucagon-like peptide 1 in the anesthetized pig. Diabetes 1998;47:764–9.
[18] Kubota N, Tobe K, Terauchi Y, Eto K, Yamauchi T, Suzuki R, et al. Disruption of insulin receptor substrate 2 causes type 2 diabetes because of liver insulin resistance and lack of compensatory beta-cell hyperplasia. Diabetes 2000;49:1880–9.
[19] Kubota N, Kubota T, Itoh S, Kumagai H, Kozono H, Takamoto I, et al. Dynamic functional relay between insulin receptor substrate 1 and 2 in hepatic insulin signaling during fasting and feeding. Cell Metab 2008;8:49–64.
[20] Kubota N, Terauchi Y, Tobe K, Yano W, Suzuki R, Ueki K, et al. Insulin receptor substrate 2 plays a crucial role in beta cells and the hypothalamus. J Clin Invest 2004;114:917–27.
[21] Rhodes CJ. Type 2 diabetes—a matter of beta-cell life and death? Science 2005;307:380–4.
[22] Shirakawa J, Amo K, Ohminami H, Orime K, Togashi Y, Ito Y, et al. Protective effects of dipeptidyl peptidase-4 (DPP-4) inhibitor against increased beta cell apoptosis induced by dietary sucrose and linoleic acid in mice with diabetes. J Biol Chem 2011;286:25467–76.
[23] Wang Q, Brubaker PL. Glucagon-like peptide-1 treatment delays the onset of diabetes in 8 week-old db/db mice. Diabetologia 2002;45:1263–73.
[24] Tourrel C, Bailbe D, Lacorne M, Meile MJ, Kergoat M, Portha B. Persistent improvement of type 2 diabetes in the Goto-Kakizaki rat model by expansion of the beta-cell mass during the prediabetic period with glucagon-like peptide-1 or exendin-4. Diabetes 2002;51:1443–52.
[25] Mu J, Woods J, Zhou YP, Roy RS, Li Z, Zycband E, et al. Chronic inhibition of dipeptidyl peptidase-4 with a sitagliptin analog preserves pancreatic beta-cell mass and function in a rodent model of type 2 diabetes. Diabetes 2006;55:1695–704.
[26] Cheng Q, Law PK, de Gasparo M, Leung PS. Combination of the dipeptidyl peptidase IV inhibitor LAF237 [(S)-1-[(3-hydroxy-1-adamantyl)ammo]acetyl-2-cyanopyrrolidine] with the angiotensin II type 1 receptor antagonist valsartan [N-(1-oxopentyl)-N-[[2′-(1H-tetrazol-5-yl)-[1,1′-biphenyl]-4-yl] methyl]-L-valine] enhances pancreatic islet morphology and function in a mouse model of type 2 diabetes. J Pharmacol Exp Ther 2008;327:683–91.
[27] Park S, Dong X, Fisher TL, Dunn S, Omer AK, Weir G, et al. Exendin-4 uses Irs2 signaling to mediate pancreatic beta cell growth and function. J Biol Chem 2006;281:1159–68.
[28] Jhala US, Canettieri G, Screaton RA, Kulkarni RN, Krajewski S, Reed J, et al. cAMP promotes pancreatic beta-cell survival via CREB-mediated induction of IRS2. Genes Dev 2003;17:1575–80.
[29] Gomez E, Pritchard C, Herbert TP. cAMP-dependent protein kinase and Ca2+ influx through L-type voltage-gated calcium channels mediate Raf-independent activation of extracellular regulated kinase in response to glucagon-like peptide-1 in pancreatic beta-cells. J Biol Chem 2002;277:48146–51.
[30] Kim MJ, Kang JH, Park YG, Ryu GR, Ko SH, Jeong IK, et al. Exendin-4 induction of cyclin D1 expression in INS-1 beta-cells: involvement of cAMP-responsive element. J Endocrinol 2006;188:623–33.
[31] Moritoh Y, Takeuchi K, Asakawa T, Kataoka O, Odaka H. Chronic administration of alogliptin, a novel, potent, and highly selective dipeptidyl peptidase-4 inhibitor, improves glycemic control and beta-cell function in obese diabetic ob/ob mice. Eur J Pharmacol 2008;588:325–32.
[32] Prentki M, Nolan CJ. Islet beta cell failure in type 2 diabetes. J Clin Invest 2006;116:1802–12.
[33] Gedulin BR, Nikoulina SE, Smith PA, Gedulin G, Nielsen LL, Baron AD, et al. Exenatide (exendin-4) improves insulin sensitivity and {beta}-cell mass in insulin-resistant obese fa/fa Zucker rats independent of glycemia and body weight. Endocrinology 2005;146:2069–76.
[34] Nauck MA. Incretin-based therapies for type 2 diabetes mellitus: properties, functions, and clinical implications. Am J Med 2011;124:S3–S18.
[35] DeFronzo RA, Okerson T, Viswanathan P, Guan X, Holcombe JH, MacConell L. Effects of exenatide versus sitagliptin on postprandial glucose, insulin and glucagon secretion, gastric emptying, and caloric intake: a randomized, cross-over study. Curr Med Res Opin 2008;24:2943–52.

JCM
Journals.ASM.org

Utility of Detection of Telaprevir-Resistant Variants for Prediction of Efficacy of Treatment of Hepatitis C Virus Genotype 1 Infection

Norio Akuta,[a] Fumitaka Suzuki,[a] Taito Fukushima,[a] Yusuke Kawamura,[a] Hitomi Sezaki,[a] Yoshiyuki Suzuki,[a] Tetsuya Hosaka,[a] Masahiro Kobayashi,[a] Tasuku Hara,[a] Mariko Kobayashi,[b] Satoshi Saitoh,[a] Yasuji Arase,[a] Kenji Ikeda,[a] Hiromitsu Kumada[a]

Department of Hepatology, Toranomon Hospital, and Okinaka Memorial Institute for Medical Research, Tokyo, Japan[a]; Liver Research Laboratory, Toranomon Hospital, Tokyo, Japan[b]

The clinical usefulness of detecting telaprevir-resistant variants is unclear. Two hundred fifty-two Japanese patients infected with hepatitis C virus (HCV) genotype 1b received triple therapy with telaprevir–peginterferon (PEG-IFN)–ribavirin and were evaluated for telaprevir-resistant variants by direct sequencing at baseline and at the time of reelevation of the viral load. An analysis of the entire group indicated that 76% achieved a sustained virological response. Multivariate analysis identified a PEG-IFN dose of <1.3 μg/kg of body weight, an *IL28B* rs8099917 genotype (genotype non-TT), detection of telaprevir-resistant variants of amino acid (aa) 54 at baseline, nonresponse to prior treatment, and a leukocyte count of <5,000/mm^3 as significant pretreatment factors for detection of telaprevir-resistant variants at the time of reelevation of the viral load. In 63 patients who showed nonresponse to prior treatment, a higher proportion of patients with no detected telaprevir-resistant variants at baseline (54%) achieved a sustained virological response than did patients with detected telaprevir-resistant variants at baseline (0%). Furthermore, 2 patients who did not have a sustained virological response from the first course of triple therapy with telaprevir received a second course of triple therapy with telaprevir. These patients achieved a sustained virological response by the second course despite the persistence of very-high-frequency variants (98.1% for V36C) or a history of the emergence of variants (0.2% for R155Q and 0.2% for A156T) by ultradeep sequencing. In conclusion, this study indicates that the presence of telaprevir-resistant variants at the time of reelevation of viral load can be predicted by a combination of host, viral, and treatment factors. The presence of resistant variants at baseline might partly affect treatment efficacy, especially in those with nonresponse to prior treatment.

New strategies have been introduced recently for the treatment of chronic hepatitis C virus (HCV) infection based on the inhibition of protease in the nonstructural 3 (NS3)/NS4 region of the HCV polyprotein. Of the new agents currently available, telaprevir (VX-950) is used for the treatment of chronic HCV infection (1). Three studies (PROVE1, PROVE2, and a Japanese study [2–4]) showed that a 24-week regimen of triple therapy (telaprevir, peginterferon [PEG-IFN], and ribavirin) for 12 weeks followed by dual therapy (PEG-IFN and ribavirin) for 12 weeks (also called the T12PR24 regimen) achieved sustained virological response (SVR) (negative for HCV RNA for >24 weeks after the withdrawal of treatment) rates of 61%, 69%, and 73%, respectively, in patients infected with HCV genotype 1 (HCV-1). However, another study (PROVE3) found lower SVR rates to the T12PR24 regimen (39%) in nonresponders to previous PEG-IFN–ribavirin therapy infected with HCV-1 who did not achieve HCV RNA negativity during or at the end of the initial triple therapy course (5).

Telaprevir-based therapy is reported to induce resistant variants of HCV (6, 7). A recent report indicated that resistant variants are observed in most patients after failure to achieve an SVR by telaprevir-based treatment and that they tend to be replaced with wild-type viruses over time, presumably due to the lower fitness of those variants (8). However, the clinical usefulness of detecting telaprevir-resistant variants is still unclear. First of all, pretreatment factors associated with the detection of telaprevir-resistant variants at the time of reelevation of viral load have not been investigated. Furthermore, it is not clear at this stage whether the detection of telaprevir-resistant variants at baseline is useful for predicting the efficacy of telaprevir-based treatment and whether a history of the emergence of telaprevir-resistant variants affects treatment efficacy with the second course of telaprevir-based treatment.

Based on the above background, there is a need to investigate the clinical usefulness of detecting telaprevir-resistant variants. The aim of this study was to determine the pretreatment factors associated with the subsequent detection of telaprevir-resistant variants at the time of reelevation of viral load and the importance of telaprevir-resistant variants for predicting the efficacy of telaprevir-based treatment in patients infected with HCV-1b.

MATERIALS AND METHODS

Study population. From May 2008 through August 2013, 340 consecutive patients infected with HCV were selected for triple therapy with telaprevir (MP-424 or Telavic; Mitsubishi Tanabe Pharma, Osaka, Japan), PEG-IFN-α2b (PegIntron; MSD, Tokyo, Japan), and ribavirin (Rebetol; MSD, Tokyo) at the Department of Hepatology, Toranomon Hospital (located in metropolitan Tokyo, Japan). Subsequently, 252 of these patients received the triple therapy based on the following inclusion and exclusion criteria: (i) diagnosis of chronic hepatitis C, (ii) HCV-1b confirmed by sequence analysis, (iii) HCV RNA level of ≥5.0 log IU/ml as determined

Received 28 August 2013 Returned for modification 22 October 2013
Accepted 26 October 2013
Published ahead of print 6 November 2013
Editor: A. M. Caliendo
Address correspondence to Norio Akuta, akuta-gi@umin.ac.jp.

doi:10.1128/JCM.02371-13

by the Cobas TaqMan HCV test (Roche Diagnostics, Tokyo, Japan), (iv) follow-up duration of ≥24 weeks after the completion of triple therapy, (v) no history of treatment with NS3/4A protease inhibitors, (vi) absence of decompensated liver cirrhosis and hepatocellular carcinoma (HCC), (vii) negative for hepatitis B surface antigen (HBsAg), (viii) no evidence of human immunodeficiency virus infection, (ix) negative history of autoimmune hepatitis, alcohol liver disease, hemochromatosis, and chronic liver disease other than chronic hepatitis C, (x) negative history of depression, schizophrenia, or suicide attempts, angina pectoris, cardiac insufficiency, myocardial infarction, severe arrhythmia, uncontrolled hypertension, uncontrolled diabetes, chronic renal dysfunction, cerebrovascular disorders, thyroidal dysfunction uncontrolled by medical treatment, chronic pulmonary disease, allergy to medication, or anaphylaxis at baseline, and (xi) pregnant or breastfeeding women or those willing to become pregnant during the study and men with a pregnant partner were excluded. The study protocol was in compliance with the guidelines for good clinical practice and the 1975 Declaration of Helsinki and was approved by the institutional review board of the Toranomon Hospital. Each patient received ample information about the goals and potential side effects of the treatment and their right to withdraw from the study at any time. Each patient provided a signed consent form before participating in this trial.

The efficacy of treatment was evaluated by the presence or absence of an HCV RNA-negative result at 24 weeks after the completion of therapy (i.e., SVR), as determined by the Cobas TaqMan HCV test (Roche Diagnostics). Furthermore, failure to achieve an SVR was classified as nonresponse (HCV RNA detected during or at the end of treatment) or relapse (at the time of reelevation of viral load after the end of treatment, even when HCV RNA result was negative at the end of treatment).

Twenty patients (8%) were assigned to a 12-week regimen of triple therapy (the T12PR12 group) and were randomly divided into two groups (10 patients each) treated with either 1,500 mg/day or 2,250 mg/day of telaprevir to evaluate the treatment efficacy during 12 weeks on treatment. Sixty patients (24%) were allocated to a 24-week regimen of the same triple therapy described above followed by dual therapy of PEG-IFN and ribavirin for another 12 weeks (the T12PR24 group) to evaluate treatment efficacy according to the response to prior treatment, and they were treated with 2,250 mg/day of telaprevir. Another group of 172 patients (68%) was treated as described above for the T12PR24 group except for the dosages of telaprevir; this group was divided into two groups treated with either 1,500 mg/day (111 patients) or 2,250 mg/day (61 patients) of telaprevir, as selected by the attending physician. Table 1 summarizes the profiles and laboratory data of the entire group of 252 patients at the commencement of treatment. They included 155 males and 97 females 21 to 73 years of age (median, 58 years). At the start of treatment, telaprevir was administered at a median dose of 30.8 mg/kg of body weight (range, 14.1 to 59.2 mg/kg) daily. One hundred thirty-one patients (52%) were treated with 2,250 mg/day of telaprevir, while the other 121 patients (48%) were treated with 1,500 mg/day of telaprevir. PEG-IFN-α2b was injected subcutaneously at a median dose of 1.5 μg/kg (range, 0.7 to 1.8 μg/kg) once a week. Ribavirin was administered at a median dose of 10.9 mg/kg (range, 4.3 to 15.8 mg/kg) daily. Each drug was discontinued or its dose reduced as required per the judgment of the attending physician, in response to a fall in hemoglobin level, leukocyte count, neutrophil count, or platelet count, or the appearance of side effects. The triple therapy was discontinued when the leukocyte count decreased to $<1{,}000/mm^3$, the neutrophil count decreased to $<500/mm^3$, the platelet count decreased to $<5.0 \times 10^4/mm^3$, or when hemoglobin decreased to <8.5 g/dl.

Follow-up. Clinical and laboratory assessments were performed at least once every month before, during, and after treatment. They were performed every week in the initial 12 weeks of treatment. Adverse effects were monitored clinically by careful interviews and a medical examination at least once every month. Compliance with treatment was evaluated by a questionnaire.

TABLE 1 Profile and laboratory data at commencement of telaprevir, peginterferon, and ribavirin triple therapy in patients infected with HCV genotype 1b

Variable	Patient data
Patient demographics	
No. of patients	252
Sex (no. of males/no. of females)	155/97
Median age (yr) (range)	58 (21–73)
Median body mass index (kg/m^2) (range)	22.8 (16.0–36.7)
Laboratory data (median [range])	
Level of viremia (log IU/ml)	6.7 (5.0–7.8)
Aspartate aminotransferase (IU/liter)	37 (15–624)
Alanine aminotransferase (IU/liter)	42 (11–525)
Albumin (g/dl)	3.9 (2.5–4.7)
Gamma-glutamyl transpeptidase (IU/liter)	34 (3–319)
Leukocyte count ($/mm^3$)	4,700 (2,000–8,400)
Hemoglobin (g/dl)	14.3 (12.1–17.6)
Platelet count ($10^4/mm^3$)	16.5 (8.5–33.8)
Treatment	
Median PEG-IFN-α2b dose (μg/kg) (range)	1.5 (0.7–1.8)
Median ribavirin dose (mg/kg) (range)	10.9 (4.3–15.8)
Median telaprevir dose (mg/kg) (range)	30.8 (14.1–59.2)
No. of patients with telaprevir dose of 1,500/2,250 mg/day	121/131
No. of patients on T12PR12/T12PR24 treatment regimen	20/232
Response to prior treatment	
No. of treatment-naive patients/no. of patients with relapse to prior treatment/no. of patients with nonresponse to prior treatment (IFN monotherapy/ribavirin combination therapy)/unknown	79/109/63 (16/47)/1
Amino acid substitutions in HCV genotype 1b	
Core aa 70 (arginine/glutamine [histidine]/ND[a])	162/88/2
Core aa 91 (leucine/methionine/ND)	139/111/2
ISDR of NS5A (wild type/non-wild type/ND)	199/24/29
IRRDR of NS5A (≤5/≥6/ND)	180/69/3
V3 of NS5A (≤2/≥3/ND)	64/185/3
IL28B genotype	
rs8099917 genotype (TT/non-TT/ND)	181/69/2
ITPA genotype	
rs112735 genotype (CC/non-CC)	186/65/1
NS3/4A protease inhibitor-resistant variants by direct sequencing[b]	
V36/T54/Q80/R155/A156/D168/V170	1/7/55/1/2/26/0

[a] ND, not determined.

[b] The NS3/4A protease inhibitor-resistant variants detected by direct sequencing included V36A/C/M/L/G, T54A/S, Q80K/R/H/G/L, R155K/T/I/M/G/L/S/Q, A156V/T/S/I/G, D168A/V/E/G/N/T/Y/H/I, and V170A (19, 20).

Measurement of HCV RNA. The antiviral effects of the triple therapy on HCV were assessed by measuring blood plasma HCV RNA levels. In this study, HCV RNA levels during treatment were evaluated at least once every month before, during, and after therapy. HCV RNA concentrations were determined using the Cobas TaqMan HCV test (Roche Diagnostics). The linear dynamic range of the assay was 1.2 to 7.8 log IU/ml, and undetectable samples were defined as negative.

Determination of *IL28B* and *ITPA* genotypes. The *IL28B* rs8099917 and *ITPA* rs112735 genotypes have been reported as predictors of treatment efficacy and side effects to PEG-IFN–ribavirin dual therapy, and they were genotyped by using the Invader assay, TaqMan assay, or direct sequencing, as described previously (9–13).

Detection of amino acid substitutions in core and NS5A regions of HCV-1b. With the use of HCV-J (GenBank accession no. D90208) as a reference type (14), the sequence of amino acids (aa) 1 to 191 in the core protein of HCV-1b was determined and then compared with the consensus sequence constructed in a previous study to detect substitutions at aa 70 of arginine (Arg70) or glutamine/histidine (Gln70/His70) and at aa 91 of leucine (Leu91) or methionine (Met91) (15). The sequence of aa 2209 to 2248 in the NS5A of HCV-1b (the interferon sensitivity-determining region [ISDR]) reported by Enomoto and coworkers (16) was determined, and the number of amino acid substitutions in the ISDR was defined as wild type (≤1) or non-wild type (≥2) compared to that of HCV-J. Furthermore, the sequence of aa 2334 to 2379 in the NS5A region of HCV-1b (the IFN/ribavirin resistance-determining region [IRRDR]) reported by El-Shamy and coworkers (17), including the sequence of aa 2356 to 2379 referred to as the variable region 3 (V3), was determined and then compared with the consensus sequence constructed in a previous study. The numbers of amino acid substitutions in the IRRDR and V3 regions were divided into two groups for analysis (those with ≤5 and ≥6 aa substitutions in the IRRDR, and those with ≤2 and ≥3 aa substitutions in the V3). In the present study, the amino acid substitutions of the core region and the NS5A-ISDR/IRRDR/V3 of HCV-1b were analyzed by direct sequencing.

Assessment of NS3/4A protease inhibitor-resistant variants. The genome sequence of 609 nucleotides (203 amino acids) in the N terminal of the NS3 region of HCV isolates from the patients was examined. HCV RNA was extracted from 100 μl of blood serum sample, and the nucleotide sequences were determined by direct sequencing and deep sequencing. The primers used to amplify the NS3 region were NS3-F1 (5′-ACA CCG CGG CGT GTG GGG ACA T-3′, nucleotides 3295 to 3316) and NS3-AS2 (5′-GCT CTT GCC GCT GCC AGT GGG A-3′, nucleotides 4040 to 4019) as the first (outer) primer pair and NS3-F3 (5′-CAG GGG TGG CGG CTC CTT-3′, nucleotides 3390 to 3407) and NS3-AS2 as the second (inner) primer pair (18). Thirty-five cycles of first and second amplifications were performed as follows: denaturation for 30 s at 95°C, annealing of primers for 1 min at 63°C, extension for 1 min at 72°C, and final extension at 72°C for 7 min. The PCR-amplified DNA was purified after agarose gel electrophoresis and then used for direct sequencing and ultradeep sequencing.

Patients were examined for NS3/4A protease inhibitor-resistant variants by direct sequencing at baseline and at the time of reelevation of viral loads. Furthermore, patients who did not have an SVR with the first course of triple therapy with telaprevir and received the second course of the triple therapy with telaprevir were analyzed for telaprevir-resistant variants by ultradeep sequencing at baseline and at the time of reelevation of viral loads. NS3/4A protease inhibitor-resistant variants included V36A/C/M/L/G, T54A/S, Q80K/R/H/G/L, R155K/T/I/M/G/L/S/Q, A156V/T/S/I/G, D168A/V/E/G/N/T/Y/H/I, and V170A. Telaprevir-resistant variants (at aa 36, aa 54, aa 155, aa 156, and aa 170) and TMC435-resistant variants (at aa 80, aa 155, and aa 168) were evaluated (19, 20).

Direct sequencing was analyzed by the Dye Terminator method. Dideoxynucleotide termination sequencing was performed with the BigDye deoxy terminator version 1.1 cycle sequencing kit (Life Technologies, Carlsbad, CA) (18). The sequence data were deposited in GenBank. Also, ultradeep sequencing was performed using the Ion Personal Genome Machine (PGM) sequencer (Life Technologies). An Ion Torrent adapter-ligated library was prepared using an Ion Xpress Plus fragment library kit (Life Technologies). Briefly, 100 ng of fragmented genomic DNA was ligated to the Ion Torrent adapters P1 and A. The adapter-ligated products were nick translated and PCR amplified for a total of 8 cycles. Subsequently, the library was purified using AMPure beads (Beckman Coulter, Brea, CA) and the concentration determined using the StepOnePlus real-time PCR (Life Technologies) and Ion Library quantitation kit, according to the instructions provided by the manufacturers. Emulsion PCR was performed using the Ion OneTouch (Life Technologies) in conjunction with the Ion OneTouch 200 template kit version 2 (Life Technologies). Enrichment for templated Ion Sphere particles (ISPs) was performed using the Ion OneTouch enrichment system (Life Technologies) according to the instructions provided by the manufacturer. Templated ISPs were loaded onto an Ion 314 chip and subsequently sequenced using 130 sequencing cycles according to the Ion PGM 200 sequencing kit user guide. The total output read length per run was >10 Mb (0.5 million tags, 200-base read) (21). The results were analyzed with the CLC Genomics Workbench software (CLC bio, Aarhus, Denmark) (22).

We also included a control experiment to validate the error rates in ultradeep sequencing of the viral genome. In this study, the amplification products of the second-round PCR were ligated with a plasmid and transformed in *Escherichia coli* by using a cloning kit (TA Cloning; Invitrogen, Carlsbad, CA). A plasmid-derived NS3 sequence was determined as the template, in a control experiment. The fold coverages evaluated per position for aa 36, aa 54, aa 155, aa 156, and aa 170 in the NS3 region were 359,379×, 473,716×, 106,435×, 105,979×, and 49,058×, respectively. Thus, using the control experiment based on a plasmid carrying the HCV NS3 sequence, amino acid mutations were defined as amino acid substitutions at a frequency of >0.2% among the total coverage. This frequency ruled out putative errors caused by the ultradeep sequence platform used in this study (23).

Statistical analysis. Nonparametric variables were compared between the groups by the chi-square and Fisher's exact probability tests. Univariate and multivariate analyses for factors affecting the presence of telaprevir-resistant variants by direct sequencing at the reelevation of viral load were performed by the chi-square test and logistic regression, respectively. Patients who achieved an SVR were said to have no detection of resistant variants at the reelevation of viral load. The sensitivity, specificity, positive predictive value (PPV), and negative predictive value (NPV) were calculated to determine the reliability of the predictors of the response to therapy.

Nucleotide sequence accession numbers. The N-terminal sequences of the NS3 regions of the telaprevir-resistant variant isolates were deposited in GenBank under accession numbers AB709241, AB709263, AB709264, AB709276, AB709279, AB709283, AB709286, AB709289, AB709295, AB709296, AB709300, AB709303, AB709307, AB709310, AB709311, AB709312, AB709317, AB709319, AB709321, AB709322, AB709345, AB709348, AB709352, AB709353, AB709354, AB709356, AB709357, AB709358, AB709360, AB709370, AB709377, AB709382, AB709383, AB709384, AB709388, AB709390, AB709392, AB709396, AB709398, AB709399, AB709401, AB709405, AB709409, AB709410, AB709414, AB709418, AB709422, AB709426, AB709437, AB709444, AB709445, AB709451, AB709456, AB709461, AB709474, AB709476, AB709481, AB709484, AB709485, AB709486, AB709488, AB709489, AB709490, AB709491, AB709492, AB709493, AB709502, AB709507, AB709508, AB709514, AB709515, AB709525, AB709526, AB709527, and AB826566 to AB826684.

RESULTS

Virological response to therapy. An analysis of the entire group showed that 76% (192 of 252 patients) achieved an SVR. According to the treatment regimen, an SVR was achieved by 45% (9 of 20 patients) and 79% (183 of 232 patients) of the T12PR12 and T12PR24 groups, respectively. Taking into consideration the response to prior treatment, an SVR was achieved by 86% (68 of 79 patients), 84% (91 of 109 patients), and 35% (32 of 63 patients) of the treatment-naive patients, patients who showed relapse following prior treatment, and nonresponders to prior treatment, respectively. In the 231 patients of the T12PR24 group, an SVR was achieved by 88% (61 of 69 patients), 85% (89 of 105 patients), and

TABLE 2 Frequencies of the subjects in whom NS3/4A protease inhibitor-resistant variants were detected by direct sequencing at baseline and at the time of reelevation of viral loads[a]

Time of variant detection	% (*n*) by aa position[b]:						
	36	54	80	155	156	168	170
Baseline	0.4 (1)	3 (7)	22 (55)	0.4 (1)	0.8 (2)	10 (26)	0 (0)
Reelevation of viral load	7 (18)	12 (30)	5 (11)	0.4 (1)	4 (10)	1.2 (3)	0.4 (1)

[a] NS3/4A protease inhibitor-resistant variants included V36A/C/M/L/G, T54A/S, Q80K/R/H/G/L, R155K/T/I/M/G/L/S/Q, A156V/T/S/I/G, D168A/V/E/G/N/T/Y/H/I, and V170A (19, 20).

[b] The data represent the percentages (*n*) of patients in whom NS3/4A protease inhibitor-resistant variants were detected by direct sequencing. Patients who achieved a sustained virological response were said to have no detection of resistant variants by direct sequencing at the time of reelevation of the viral load.

56% (32 of 57 patients) of the treatment-naive patients, patients who showed relapse following prior treatment, and nonresponders to prior treatment, respectively. Furthermore, an SVR was achieved by 86% (12 of 14 patients) and 47% (20 of 43 patients) of the nonresponders to prior IFN monotherapy and ribavirin combination therapy, respectively.

NS3/4A protease inhibitor-resistant variants detected by direct sequencing at baseline and at the time of reelevation of viral loads. All of the 252 patients were evaluated for resistant variants by direct sequencing at baseline. Sixty patients who did not achieve an SVR were also analyzed for resistant variants by direct sequencing at the time of reelevation of viral load. One hundred ninety-two patients who achieved SVR were said to have no detection of resistant variants as determined by direct sequencing at the reelevation of viral load.

As a whole, the frequency of the subjects in whom telaprevir-resistant variants were detected increased from 5% (12 of 252 patients) at baseline to 18% (45 of 252 patients) at the time of reelevation of viral load. On the other hand, the frequency of the subjects in whom TMC435-resistant variants were detected decreased from 31% (78 of 252 patients) at baseline to 6% (14 of 252 patients) at the time of reelevation of viral load. Table 2 shows the frequencies of subjects in whom resistant variants were detected at baseline and at the time of reelevation of viral load per position for aa 36, aa 54, aa 80, aa 155, aa 156, aa 168, and aa 170 in the NS3 region.

Pretreatment factors associated with detection of telaprevir-resistant variants by direct sequencing at the time of reelevation of viral load. Univariate analysis of the data of the entire group identified eight pretreatment factors that were significantly associated with the detection of telaprevir-resistant variants by direct sequencing at the time of reelevation of viral load: *IL28B* rs8099917 genotype (genotype non-TT) ($P < 0.001$), nonresponse to prior treatment ($P < 0.001$), PEG-IFN dose of <1.3 μg/kg ($P = 0.001$), detection of variants at aa 54 at baseline ($P = 0.002$), Gln70/His70 substitution of aa 70 ($P = 0.003$), gamma-glutamyl transpeptidase (GGT) level of ≥50 IU/liter ($P = 0.006$), leukocyte count of <5,000/mm^3 ($P = 0.026$), and ribavirin dose of <8.0 mg/kg ($P = 0.026$). Multivariate analysis that included the above variables identified five pretreatment factors that were independently associated with the detection of telaprevir-resistant variants at the time of reelevation of viral load: PEG-IFN dose of <1.3 μg/kg (odds ratio [OR], 9.71; $P < 0.001$), *IL28B* rs8099917 genotype (genotype non-TT) (OR, 8.61; $P < 0.001$), detection of variants at aa 54 at baseline (OR, 33.4; $P = 0.002$), nonresponse to prior treatment (OR, 2.66, $P = 0.018$), and leukocyte count of <5,000/mm^3 (OR, 2.46; $P = 0.042$) (Table 3).

Prediction of treatment efficacy by the combination of response to prior treatment and presence of telaprevir-resistant variants by direct sequencing at baseline. The SVR rates based on the combination of response to prior treatment and the presence of telaprevir-resistant variants by direct sequencing at baseline are shown in Fig. 1. In 79 treatment-naive patients, the SVR rates were not different between those patients in whom there were no detected telaprevir-resistant variants (86% [65 of 76 patients]) and those in whom variants were detected (67% [2 of 3 patients]). In 109 patients who showed relapse following prior treatment, the SVR rates were not different between those patients in whom there were no detected variants (83% [86 of 104 patients]) and those in whom variants were detected (100% [5 of 5 patients]). In contrast, in 63 patients who showed nonresponse to prior treatment, a higher proportion of patients with undetected telaprevir-resistant variants (54% [32 of 59 patients]) achieved an SVR than did patients in whom telaprevir-resistant variants were detected (0% [0 of 4 patients]) ($P = 0.053$). Thus, with the combination of nonresponse to prior treatment and detection of telaprevir-resistant variants, the sensitivity, specificity, PPV, and NPV for those with non-SVR were 7% (4 of 60 patients), 100% (191 of 191 patients), 100% (4 of 4 patients), and 77% (191 of 247 patients), respectively. These results indicated that the use of the combination of the above two factors has high specificity and PPV for the prediction of a non-SVR.

TABLE 3 Multivariate analysis of factors associated with detection of telaprevir-resistant variants by direct sequencing at the reelevation of viral load, to telaprevir, peginterferon, and ribavirin triple therapy in patients infected with HCV genotype 1b

Detection factors	Category	Odds ratio (95% CI[a])	*P*[b]
PEG-IFN-α2b dose (μg/kg)	≥1.3	1	
	<1.3	9.71 (3.23–29.4)	<0.001
IL28B rs8099917 genotype	TT genotype	1	
	Non-TT genotype	8.61 (3.48–21.3)	<0.001
Variants of aa 54 at baseline	No detection	1	
	Detection	33.4 (3.77–295)	0.002
Response to treatment	Naive or relapse	1	
	Nonresponse	2.66 (1.18–5.96)	0.018
Leukocyte count (/mm^3)	≥5,000	1	
	<5,000	2.46 (1.03–5.85)	0.042

[a] CI, confidence interval.

[b] Only variables that achieved statistical significance ($P < 0.05$) on multivariate logistic regression analysis are shown.